The Pennsylvania State University

The Graduate School

Neuroscience Graduate Program

LOCALIZATION AND FUNCTIONALITY OF ION CHANNELS PRESENT IN THE *DROSOPHILA MELANOGASTER* AXON INTIAL SEGMENT

A Thesis in

Neuroscience

by

Laura Glatzer

Submitted in Partial Fulfillment
of the Requirements
for the Degree of

Master of Science

May 2019

The thesis of Laura Glatzer was reviewed and approved* by the following:

Timothy Jegla
Associate Professor of Biology
Thesis Advisor

Melissa Rolls
Professor of Biochemistry and Molecular Biology

Kevin Alloway
Distinguished Educator, College of Medicine
Professor, Neural and Behavioral Sciences
Co-Director, Graduate Program in Neuroscience
Graduate Program Chair

*Signatures are on file in the Graduate School

ABSTRACT

It is well established that vertebrate species use giant-Ankryin (Ank) as a major protein responsible for maintaining a barrier for the axon initial segment (AIS), which leads to the congregation of voltage-gated sodium, calcium, and potassium channels (Jenkins et al., 2015). These ion channels help with action potential (AP) generation and regulation in the AIS, which is known to generate APs and act as a barrier to keep somato-dendritic proteins out of the axon in vertebrates (Jones & Svitkina, 2016; Nelson & Jenkins, 2017). A recent study showed that a putative Ank2-dependent AIS is present in *Drosophila* sensory neurons, meaning a putative giant-ankyrin dependent AIS formed in a common bilaterian ancestor, earlier than previously assumed (T. Jegla et al., 2016). This thesis illustrates the localization of voltage-gated potassium channels (dmElk channels) and voltage-gated calcium channels (Cacophony channels) in the putative AIS and looks at the Ank2 and discs large (Dlg) scaffolding protein effect on localization of dmElk channels through fluorescent microscopy in *Drosophila melanogaster*. Using *Drosophila melanogaster* provides an *in vivo* model with powerful genetic tools to analyze the mechanisms of AIS formation and regulation, which may prove insightful to vertebrate processes.

dmElk and the human ortholog Elk1 channels' properties were analyzed through electrophysiology experiments using two-electrode voltage clamp. The experiments showed evidence that both channels activate at hyperpolarized voltages, suggesting they contribute to the regulation of subthreshold excitability. The mechanism behind the regulation of gating properties associated with Elk1 was looked at through the application of heme and zinc on the Elk1 channel. It was observed that heme causes a left shift of the channel's gating properties allowing it to open at more hyperpolarized voltages. Meanwhile, zinc caused a right-shift suggesting a block of the channel, preventing it from opening until depolarized voltages are reached, by altering the extracellular charge clusters on S2 and S3 segments of the voltage sensors, preventing the

stabilization of S4 segment that controls the level of block in the pore. The combination of zinc and heme caused the farthest right-shift resulting in the hypothesis that heme potentiates zinc, effectively sensitizing the channel to zinc, through the deprotonation of an external charge cluster. It is important to look at heme and zinc's effects on activation of channels as tools to help us illustrate potential mechanisms behind the regulation of gating voltage-gated potassium channels. While heme and zinc are not directly at play in the physiological sense, understanding how they impact the channels may allow us to better understand what physiological conditions help regulate channel activation and ultimately action potential generation.

TABLE OF CONTENTS

LIST OF FIGURES

LIST OF TABLES

ACKNOWLEDGEMENTS

Throughout the last four years I have had the amazing experience of working in Dr. Timothy Jegla's lab. I have had the opportunity to work with and learn from many great people throughout my time in his lab and my project's collaboration with Dr. Melissa Roll's lab. I can't thank Dr. Rolls and Dr. Jegla enough for their guidance in my research over my time in their labs. I also want to thank the many undergraduate and graduate students in my lab that I have become friends with and are always willing to talk through any issues that came up through my research. Working in Dr. Jegla's lab not only provided me with a strong science background but also an amazing mentor who is always willing to talk about any and all topics. I have had so much fun and learned so much during my time in this lab and will always be grateful to Dr. Jegla for this opportunity.

I also have been lucky to be able to take some fascinating Neuroscience classes and learn so much about the field that goes well beyond my research. Dr. Alloway has been a fantastic instructor that has pushed me to try my absolute hardest and get the most out of my time at Penn State. I will always look up to him and aspire to have his work ethic.

Finally I'd like to thank my family and friends- especially Emily, Kylie, Chris, and Andrew- for their support throughout my time at Penn State and listening to me rant on numerous occasions about my research. They helped keep me stay calm when the going got rough and for that I am indebted to them.

Funding for this research was supported by the NSF: EAGER 1621027 Plant Sensory Perception via Heme Modulation of K+ Channels TJ and SMA grant, NIH: 1 R21 NS093477 A Simple, Genetically Tractable Model for Axon Initial Segment Function MMR and TJ grant, and Eberly College of Science Undergraduate Research Grant. Any opinions, findings, and

conclusions or recommendations expressed in this publication are those of the author and do not necessarily reflect the views of the NSF and NIH awarding agencies.

Chapter 1

Introduction

The Scope of This Thesis

The nervous system is crucial to the function of most species. For that reason, many current biological questions are within the field of neuroscience However, many parts of the nervous system are not well understood. This aim of this research is to further scientific knowledge of the nervous system by investigating a region of the basic neuronal unit, the neuron, and the channels found there. The region studied, the axon initial segment (AIS), is crucial for the production and regulation of action potentials (APs), which propagate down axons and assist in sending signals from one neuron to the next. Voltage-gated ion channels are required for regular action potential regulation and are predominantly located in the AIS and nodes of Ranvier. The cellular and molecular biology of this important region has been studied in cultured mammalian neurons. However, the question mainly remains of how the AIS functions and is regulated *in vivo*, which is addressed in this study through the model organism *Drosophila melanogaster* by using larval sensory neurons that can be visualized *in vivo* at subcellular resolutions.

Using this model this research demonstrates the presence of voltage-gated potassium (dmElk) and voltage-gated calcium (Cac) channels in the putative AIS of *Drosophila melanogaster*. The study also supplies functional data for the *Drosophila* Elk channel (dmElk) and its human ortholog Elk1 (Kv12.1). Heme and zinc were used during electrophysiological readings as tools to begin to form a hypothesis as to how the gating of the Elk1 channel is regulated. The localization of the channels was determined using fluorescent microscopy under physiological conditions and under conditions where the anchoring proteins Ankyrin and Discs

large were knocked down. The dmElk and Elk1 channel properties were determined through standard two-electrode voltage clamp electrophysiological techniques in standard pH 7, 7.5, or 8 solutions, varying concentrations of heme solutions (300nM-10μM), and 300μM zinc solutions to help determine gating principles.

Overall the aim of this thesis is to first illustrate the localization of various channels and the mechanism behind this localization in the crucial region of the axon called the AIS and secondly determining if the potassium channels in this region could have similar subthreshold functions as their mammalian ortholog. The research then went one step further to look at the Elk1 mammalian ortholog to determine how the regulation of this channel and therefore of subthreshold excitability maintenance may be controlled.

Axon Initial Segment (AIS)

Structure of the Mammalian AIS

This axon initial segment (AIS) is the region of the neuron found on the axon proximal to the soma, covering approximately 20-60 μm of the axon and is bordered by various proteins that help localize specific channels to the region by creating a diffusion barrier (Jones & Svitkina, 2016). The diverse collection of proteins are specialized to three different levels within the mammalian AIS: the plasma membrane, submembrane cytoskeleton, and inner AIS shaft (Figure 1-1) (Jones & Svitkina, 2016).

The plasma membrane of the mammalian AIS has been shown to contain cell-adhesion molecules (CAMs) and voltage-gated ion channels that are crucial for action potential generation and regulation: including voltage-gated sodium, calcium, and potassium channels (similar to the Elk channels discussed throughout this thesis) (Jones & Svitkina, 2016; Kole et al., 2008).

Evidence has been found that a motif in the linker protein between domains I and II in the α subunit of voltage-gated sodium channels is responsible for giant-Ankyrin (AnkG) binding in the cytoplasm and the channels' subsequent localization (Garrido et al., 2003; Lemaillet, Walker, & Lambert, 2003). Voltage-gated potassium channels in the Kv7 family were shown to bind to AnkG in the same way as NaV channels due to a conserved motif found in both channels (Pan et al., 2006). Kv1 channels however, are localized in clusters on the surface of the membrane by the scaffolding protein PSD-93 (Ogawa et al., 2008). This variety of localization for different types of Kv channels raises the question of which protein is responsible for Elk channels in the *Drosophila* AIS. Cav2 and Cav3 voltage-gated calcium channels similar to the Cacophony channel discussed in this thesis have been shown to co-localize with potassium channels (Jones & Svitkina, 2016).

Interestingly, scaffolding proteins that hold the aforementioned channels or CAMs in place, are partially found in the submembrane level, including the N-terminus of the AnkG protein (Jones & Svitkina, 2016). AnkG then acts to recruit the protein βIV-spectrin to the AIS through a shared binding region (Davis et al., 2009; Yang, Ogawa, Hedstrom, & Rasband, 2007). βIV-spectrin then helps maintain the structure of the AIS as well as participates in recruitment of the ion channels and CAMs located in the plasma membrane of the regions (Bennett & Baines, 2001; Berghs et al., 2000). Finally, the submembrane level of the AIS seems to localize actin to some extent; however, it appears sparsely and mostly seems to maintain structure of the region or potentially has some kind of remodeling functions(Jones, Korobova, & Svitkina, 2014).

AnkG has previously been mentioned in the plasma membrane and submembrane levels of the AIS, but its C-terminal is also found in the third level of the AIS, the inner AIS shaft (Leterrier et al., 2015). The fact that AnkG is found in all three levels of the AIS shows its importance in the structure and ultimately function of the region. Although not crucial for our discussion of the AIS in this work, the inner shaft has also been shown to contain microtubules,

actin, and neurofilaments all helping determine polarity and structure of the axon (Palay, Sotelo, Peters, & Orkand, 1968; Xu, Zhong, & Zhuang, 2013).

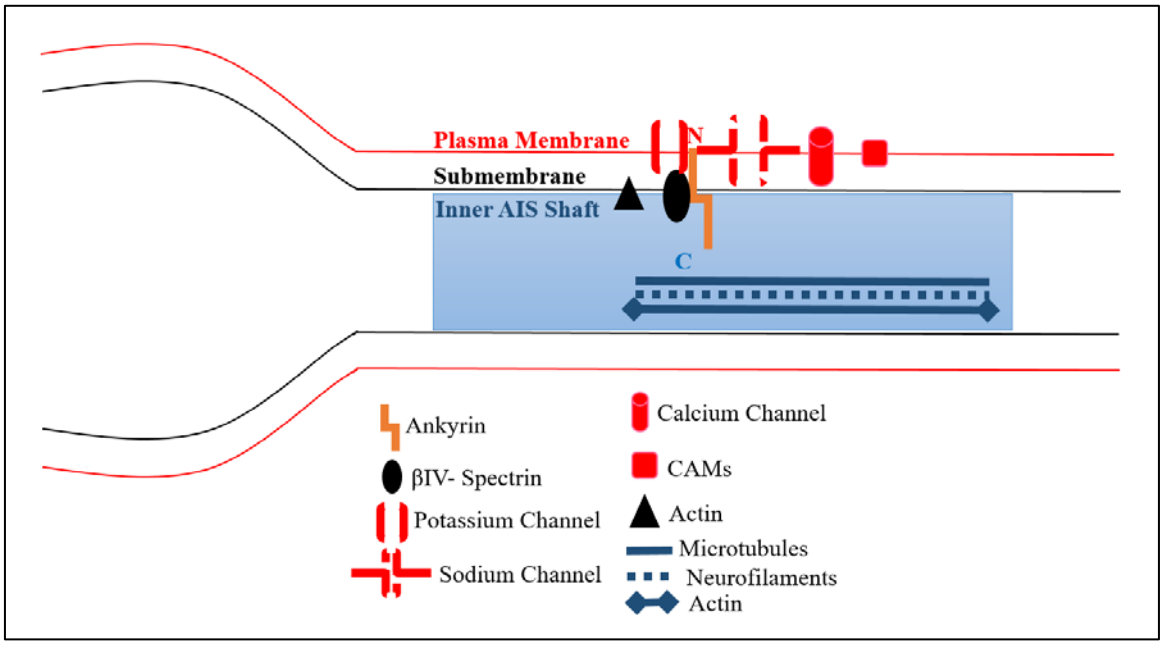

Figure 1-1: Schematic of the Structure of the Mammalian Axon Initial Segment.
This image shows a simple schematic of the structure of the mammalian AIS, while not complete in all details of the region it illustrates where the major proteins are located

Function of the Mammalian AIS

Many of the proteins that make up the structure of the AIS are crucial for the region to attend to its specific functions: action potential generation and polarity maintenance. The following section will discuss what is meant by those functions and what proteins are involved. It is important to note that these functions have been confirmed in the mammalian AIS but are assumed to be similar in the *Drosophila* putative AIS.

Action Potential Generation

In vertebrates, the axon initial segment (AIS) has been shown to be the point of action potential (AP) generation (Bender & Trussell, 2012; Nelson & Jenkins, 2017). Potassium channels are present in the AIS region to help keep the neuron at its resting potential and maintain the threshold voltage. One way this is done is through the integration of various depolarizations, preventing random spikes in the axon, by Kv1 channels which help determine the duration of the spike in axons (Kole, Letzkus, & Stuart, 2007; Shu, Yu, Yang, & McCormick, 2007). Voltage-gated sodium channels allow the cell to depolarize at the AIS, which then leads to an all-or-none action potential firing, following increased membrane potentials (Kole et al., 2008). The voltage-gated sodium channels inactivate at the peak of depolarization and the voltage-gated potassium channels that start to open just before threshold voltage, such as Kv7 channels, lead to the return of the cell to resting membrane potential and help regulate the threshold voltage (Shah, Migliore, Valencia, Cooper, & Brown, 2008). Understanding the function of channels that open at different voltages leads to the question of what dmELK could be doing in the putative AIS if the same principles of voltage activation levels are followed. Cacophony (voltage-gated calcium) channels are also of interest as to if they are in the putative *Drosophila* AIS since they have been shown in mammals to help regulate action potential generation and timing potentially through an increase in depolarization (Bender & Trussell, 2009).

Polarity Maintenance

The structural proteins previously discussed, such as AnkG, help stabilize the AIS allowing it to maintain polarity of the neuron by allowing compartmentalization between the somatodendritic and axonal compartments (Rasband, 2010; M. M. Rolls, 2011). AnkG and other

proteins help form a diffusion barrier, which prevents ion channels and other proteins from different regions from mixing together, helping to form distinct compartments with specific functions (Brachet et al., 2010; Winckler, Forscher, & Mellman, 1999). There is also evidence that suggests when proteins do make it to the AIS they are immobilized in part due to the inability of phospholipids to diffuse across the region and only certain proteins are selectively filtered across the region (Kobayashi, Storrie, Simons, & Dotti, 1992; Nakada et al., 2003; Song et al., 2009). This polarity maintenance is crucial for the AIS to initiate the directionality of action potential propagation towards axonal synapses (Rasband, 2010).

Evolution

Until recently, most research pointed towards the idea that a giant-Ankyrin dependent AIS only evolved after the bilaterian divergence. Giant-Ankyrin (AnkG) was found as a new gene in vertebrates and was believed to be the product of two subsequent gene duplications (Kordeli, Lambert, & Bennett, 1995). It was termed AnkG due to its giant 480kDa isoform that has a large binding domain for spectrin and multiple voltage-gated ion channels (Kordeli et al., 1995). The suggestion has since arose that the ability for AnkG and spectrin to bind and efficiently recruit ion channels to the AIS is reflective of the vertebrate evolution of fast, precise signaling through the control of action potential generation (Bennett & Lorenzo, 2013; Jenkins et al., 2015). Further evidence for this later evolution of the giant ankyrin-dependent AIS came about as it was shown voltage-gated sodium channels known to localize with AnkG were first found in the earliest vertebrates and voltage-gated potassium channels localized to AnkG, KCNQ2 (Kv7), were found in chordates, shortly after the split from early vertebrates (Hill et al., 2008).

However, some other evidence suggested that the AIS had to have evolved prior to the divergence of bilaterians. For example, most types of voltage-gated potassium channels, many of

which are involved in action potential regulation in the AIS, originated in metazoans prior to the bilaterian divergence (T. Jegla, Grigoriev, Gallin, Salkoff, & Spencer, 1995; T. Jegla et al., 2012; T. Jegla & Salkoff, 1994; Li, Liu, et al., 2015; Li, Martinson, et al., 2015). Additionally, *Drosophila*, vertebrates, have distinct neuronal polarity resulting in dendrites and axons suggesting the need for an AIS-like structure to help maintain this polarity (M. M. Rolls, 2011). A recent study by our lab found a giant-Ankyrin dependent putative AIS in a sensory neuron in *Drosophila*, a protostome, suggesting a common bilaterian ancestor as the origin of the giant-Ankyrin dependent AIS (T. Jegla et al., 2016). This study followed the discovery of an AIS-like segment in a mushroom body neuron (Trunova, Baek, & Giniger, 2011). The giant-ankyrin looked at in this thesis, Ank2, has previously been associated with synaptic stability at the neuromuscular junction in *Drosophila* mostly through an interaction with microtubules (Koch et al., 2008; Pielage et al., 2008). Ank2 has both an XL and L exon, categorizing it as a giant-ankyrin, and has recently been shown to be responsible for anchoring Shal, a voltage-gated potassium channel, in the putative AIS of *Drosophila* (T. Jegla et al., 2016). Evidence has been shown that the putative AIS also contains the dmElk channel; however, no information regarding the mechanism of localization of this channel has been presented, a concept this thesis delves into further (T. Jegla et al., 2016).

Finding this earlier evolution, allows the use of a strong genetic model organism, *Drosophila*, to further understand the AIS and its formation in invertebrates and relate this information to vertebrates where similar genetic modification experiments are not as easily performed.

Overview of Relevant Voltage-Gated Ion Channels

Voltage-gated Potassium Channels

Evolution of Elk Channels

Voltage-gated potassium channels are responsible for the efflux of potassium ions across a cell membrane once a certain voltage is reached. It has been shown that three gene families code for animal voltage-gated potassium channels: Shaker, KCNQ, and ether-a-go-go (EAG) (Li, Liu, et al., 2015). Shaker channels, which derived in basal metazoans, are subdivided into four subfamilies- Shaker, Shab, Shal, and Shaw- which have multiple suggested functionalities including neuronal repolarization in part due to their unique subunit structure with a pore and a family specific domain in the cytoplasm (Li, Liu, et al., 2015). KCNQ channels lack the cytoplasmic domain of the Shaker channels but have another family specific motif with high amino-acid conservation that may contribute to their assembly and ability to regulate subthreshold excitability (Li, Liu, et al., 2015). Shaker, KCNQ, and EAG (discussed below) channels have all been found in cnidarians, providing evidence that they evolved prior to the divergence of bilaterians (T. J. Jegla, Zmasek, Batalov, & Nayak, 2009; Li, Liu, et al., 2015).

EAG Super Family Channels

Voltage-gated potassium (K^+) channels classified in the ether-à-go-go (EAG) superfamily include the gene subfamilies Eag, Erg, and Elk, which differ by sequence and functionality (Li, Martinson, et al., 2015). While all of these channels show high conservation across evolution, we are most interested in the Elk channels, which have been highly conserved in a manner that causes them to activate at hyperpolarized voltages (Li, Liu, et al., 2015). This is crucial in

regulating action potentials since the neuron needs to be able to reach a certain threshold voltage before being able to fire, which is in part inhibited by the efflux of potassium. We are interested in how they can be activated at these hyperpolarized voltages and what can regulate this activation.

In regards to the channel localization data presented within this thesis the channel will be referred to as dmElk since in *Drosophila melanogaster* there is only one gene that codes for the channel, the locus of which is found on the right arm of the second chromosome in the polytene chromosome region 54F3-55A2 (Frolov, Bagati, Casino, & Singh, 2012; Warmke & Ganetzky, 1994). When electrophysiology data is discussed we will refer mostly to the human Kv12.1 channel, called Elk1. Elk1, is one of three genes that code for the Elk channel in mammals due to gene duplications in the vertebrate lineage (Giovane, Sobieszczuk, Mignon, Mattei, & Wasylyk, 1995; Harindranath, Mills, Mitchell, Meindl, & Max, 1998). Elk1 was chosen over Elk2 and Elk3 due to its higher expression levels and lack of inactivation properties. These higher expression levels allow us to get currents that are significantly higher than noise and native currents. Additionally, since we were most concerned with activation of channels we wanted to ensure that inactivation properties did not impact the way we were able to look at activation of channels.

Evidence of Elk Channel Localization and Functionality

Our lab has found evidence that Elk channels (dmElk) are localized in the AIS region of larval sensory neurons in *Drosophila* (T. Jegla et al., 2016). It is important to elucidate the channel's localization, the process behind localization, and the function of the channel, which based on prior research this is likely to be involved in maintaining subthreshold excitability (Li, Anishkin, et al., 2015; Li, Martinson, et al., 2015; Zhang et al., 2010). To help determine all of these topics, the following research used an *in vivo* model through the creation of *Drosophila*

genetic mutants and taking images of the first-generation larva which were fluorescently-marked. Using *Drosphila* allows us to better understand how Elk channels may help regulate action potentials, under the assumption that different Elk channels have the same properties.

Previous research has focused the bulk of gating data on the Kv12.2, Elk2 channel, which is coded for by the Elk2 gene (Zhang et al., 2010). Electroencephalography was used on mice models with Kv12.2 deletions to see how the lack of Kv12.2 channels would impact the ability to fire action potentials (Zhang et al., 2010). An increased amount of seizures in these mutant mice showed that these Kv12.2 voltage-gated potassium channels are responsible for maintaining threshold voltages and preventing hyperexcitability through subthreshold excitability regulation in mammalian neurons (Zhang et al., 2010).

Our research delves into the gating properties of the human Elk1 channel. Elk1, with a highly conserved low threshold voltage, was used over other Elk channels due to its high RNA expression levels in oocytes, allowing ideal current size, and lack of inactivation properties (Li, Anishkin, et al., 2015). The functional gating properties of the *Drosophila melanogaster* Elk and its human counterpart were characterized using two-electrode voltage clamp to observe the voltages at which the channels opened.

Voltage-gated Calcium Channels (Cacophony)

Localization and Suggested Function of Cac Channels

Cacophony channels (Cac) are well-characterized in their regulation of neurotransmitter release from the presynaptic neuron, but are also localized in the AIS region (Astorga et al., 2016; Lee, Ueda, & Wu, 2014; Stoler & Fleidervish, 2016). The presence of discs large localized Cac channels at the synapse seem to be in part responsible for synaptic growth (Astorga et al., 2016;

Rieckhof, Yoshihara, Guan, & Littleton, 2003). At the AIS, voltage-gated calcium channels have been shown to increase calcium current, membrane depolarization, and calcium activated-potassium current (Peng & Wu, 2007). The increase in membrane depolarization due to the influx of calcium ions helps lower neuronal threshold values (Stoler & Fleidervish, 2016). This easier depolarization, in part generated by the co-localization of calcium and sodium channels, helps regulate action potentials through changes in their timing and pattern as action potentials are initiated with less sensory input to the AIS (Bender & Trussell, 2009; Stoler & Fleidervish, 2016). There is also some evidence that calcium entering the cell through voltage-gated calcium channels may act through a signaling cascade to activate calcineurin, which may then play a role in AIS plasticity, a potentially important part of action potential regulation and neuronal polarity (Evans et al., 2013; Stoler & Fleidervish, 2016). The Cac channeled looked in the following research has been shown to be a ortholog to the mammalian N-type calcium channel (Saras & Tanouye, 2016). This thesis looked at the fluorescently tagged Cac channel to help understand through our in vivo model how the generation of action potentials may be generated in the putative *Drosophila* AIS.

Chapter 2

Techniques to Investigate Ion Channel Localization Within the *Drosophila melanogaster* AIS

Localization

As previously mentioned, throughout neurons there are many types of proteins, many of which are segregated presumably by the AIS within the axon, soma, or dendrite (Jones & Svitkina, 2016; M. M. Rolls, 2011; Winckler et al., 1999). One type of protein found at the AIS is anchoring proteins. These anchoring proteins are attached at the cell membrane and bind to other proteins to keep the entity in a specific location. In our case, we look at the localization of the dmElk and Cac channels and how the anchoring proteins Ank2 and discs large (DLG) localize dmElk.

A large part of the AIS's function involves the regulation of action potentials by maintaining a threshold voltage level, which in mammals is partly performed by channels in the Kv12 family of voltage-gated potassium channels (Zhang et al., 2010). Previous data from our lab showed that dmElk channels are found in the putative AIS region, suggesting they may play a similar role in regulating subthreshold excitation (T. Jegla et al., 2016). The aim of this thesis is to quantify the *Drosophila* ortholog of the Elk1 channel's localization and determine which proteins may play a role in this location.

Understanding the complexity and functionality of the AIS involves the mapping of all ion channels present in the region. Therefore, this research started that process by also looking at how the voltage-gated calcium channel Cacophony (Cac) is localized. This channel was chosen

due to availability of a GFP-tagged genetic tool available in *Drosophila* and its potential in regulating action potentials in the AIS (Bender & Trussell, 2009; Peng & Wu, 2007).

Giant- Ankyrin in *Drosophila* (Ank2)

As previously discussed, Ank2 is a giant-ankyrin isoform of the anchoring protein ankyrin with XL and L long exons found in *Drosophila* (T. Jegla et al., 2016). This protein is believed to help maintain the boundaries of the AIS and keep channels and other proteins localized to the region (T. Jegla et al., 2016). Originally it was believed that a giant-ankyrin dependent AIS evolved after the divergence of bilaterians; however the presence of the *Drosophila melanogaster* ankyrin-dependent putative AIS provides evidence for a common ancestor, prior to this bilaterian split, having the giant isoform dependent AIS (Bennett & Lorenzo, 2013; T. Jegla et al., 2016). Due to the evidence of ion channels in mammals being dependent on AnkG and Shal being showed to localized with Ank2 in *Drosophila*, the research presented here knocked out Ank2 to see how the localization of dmElk might depend on Ank2, giving a clearer picture of the putative AIS in *Drosophila* (Garrido et al., 2003; T. Jegla et al., 2016; Nelson & Jenkins, 2017).

Discs Large (DLG) in *Drosophila*

Discs large (DLG) was first discovered in *Drosophila* as a tumor suppressor protein that co-localized with Scrib and Lgl tumor suppressor proteins (Albertson & Doe, 2003; Woods, Hough, Peel, Callaini, & Bryant, 1996). In addition to controlling cell proliferation, Dlg has been shown to help direct cell polarity mostly at junction sites and through the maintenance of the cell's cytoskeleton (Bilder, Li, & Perrimon, 2000; Woods et al., 1996). Therefore while not

directly suggested in previous research it is possible that Dlg could be involved in the maintenance of the AIS, which is crucial for neuronal polarity. Some evidence shows this as a possibility due to Dlg being localized near the axonal membrane or inside the shaft of the axon (Gan & Zhang, 2018). However, most studies point to Dlg localizing at post-synaptic cell to help localize glutamate receptors and form functional junctions (Chen & Featherstone, 2005; Hough, Woods, Park, & Bryant, 1997; Wang et al., 2011). Recent evidence has been presented suggesting Dlg has a presynaptic role in localizing Cac channels (Astorga et al., 2016). The fact that Dlg has cell polarity regulatory functions and helps localize Cac outside of the AIS makes it a point of interest in our study to see if it may also play a role in the AIS's maintenance of polarity and how it may impact other channels in the region, such as dmElk.

In vivo Model

Importance of This Type of Model

As previously mentioned, most AIS studies have looked at this area in cultured neurons; however, it is important to be able to look at this region in an *in-vivo* setting using direct observation of neurons and the use of genetic tools to observe how this critical region is naturally set-up and functioning(M. M. Rolls et al., 2007). This research uses *Drosophila melanogaster* as an *in-vivo* model by imaging live first-generation larva of various crosses to obtain proper fluorescent marking and, when appropriate, proper knockdowns.

Drosophila melanogaster

Using *Drosophila melanogaster* as an invertebrate model to look at vertebrate neurodegeneration, development, polarity, and many other topics in various genetic mutation backgrounds has been common practice for over 100 years due to the easy usability of the model (Bellen, Tong, & Tsuda, 2010; Beller & Oliver, 2006).

When looking for a model animal, scientists tend to want animals with a quick life cycle, cheap maintenance, and large amounts of off spring, all of which *Drosophila* have. In 25ºC conditions, *Drosophila* have an egg-larval period of approximately 5 days allowing quick turnaround for when larval imaging studies can be done from the point of crossing lines, as done in this study (M. Rolls). Each female *Drosophila* has been shown to lay between 30-50 eggs a day, resulting in high amounts of larval offspring allowing increased experimental numbers (Panchal & Tiwari, 2017). Importantly, the entire *Drosophila* genome has been sequenced resulting in the possibility of making direct genetic mutations that often have phenotypic changes (Debattisti & Scorrano, 2013; Panchal & Tiwari, 2017; Tardi, Cook, & Edwards, 2012). These characteristics facilitated this research in making genetic changes to determine the localization of various channels in the AIS.

Class I ddaE Sensory Neuron

The specific neuron imaged in this study was the class I ddaE sensory neuron. This sensory neuron is part of the peripheral nervous system of *Drosophila* and is found along the dorsal side of the central axis of the body of the *Drosophila* larva (Karim & Moore, 2011). DA (dendritic arborization) neurons are classified based on the complexity of their dendritic arbors,

class I neurons like the ddaE neuron have the least dendritic arborization of all four classes and also have a distinct morphology (Figure 1-2) (Grueber, Jan, & Jan, 2002; Karim & Moore, 2011).

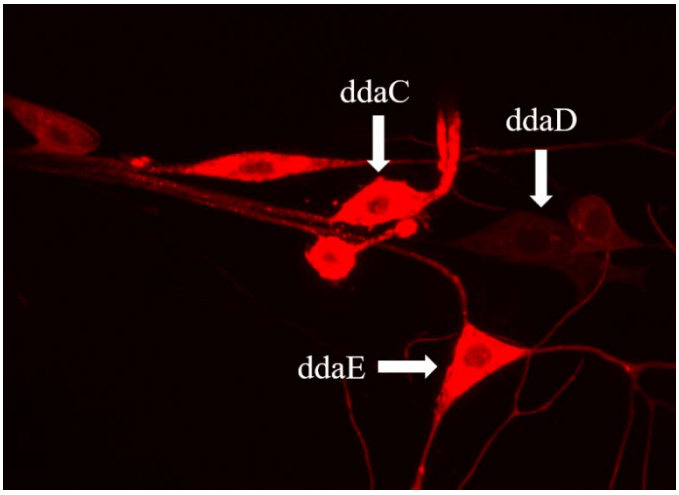

Figure 2-1: Representation of Various Neuronal Types in an IGI-mCD8-RFP Background.
This figure illustrates three types class I of DA neurons found in Drosophila. The ddaE neuron was used for all localization data.

Genetic Alterations in *Drosophila melanogaster*

Pre-existing Lines Used for Controls

All pre-existing lines were obtained from the stocks of Dr. Melissa Rolls of which lines were made by the lab, provided by other labs, or received from the Bloomington *Drosophila* Stock Center (http://flystocks.bio.indiana.edu/) or Vienna *Drosophila* RNAi Center (http://stockcenter.vdrc.at/) (T. Jegla et al., 2016).

When imaging the ddaE neuron it was crucial to be able to see the full neuron and not just the localization of the channels to ensure they imaging was of the correct class of neuron. Therefore, the plasma membrane of neuron was labelled by expressing UAS-mCD8-RFP with IGI-Gal4. UAS is the binding site for the transcription factor Gal4, which will drive the expression in class I neurons as it is attached to IGI (M. Rolls). Since mCD8-RFP, a red

fluorescent protein tag, follows UAS the RFP will be expressed in these class I neurons (M. Rolls).

When imaging the dmElk channel, UAS-Elk-GFP 5-2-2(2) was expressed with IGI-mCD8-RFP. This ensured that class I neuronal membranes were tagged with RFP and dmElk channels in the class I neurons were tagged with GFP, green fluorescent protein, on the second chromosome. Images resulting from this cross were used as a control for Elk in an Ank2 mutant background.

When imaging the dmElk channel for controls relating to a Dlg knockdown the Dicer2, mCD8-RFP; 221- Gal4, Elk1-GFP/TM6 line was expressed with y-tubulin37C RNAi (VDRC #225271). This cross expressed dmElk on the third chromosome and allowed the technique of RNAi to be used, see below.

2,3 Genetic Ankyrin Mutants

Experiments involving Ank2 mutants used lines generated with UAS-ELK-GFP balanced with TM6 on the third chromosome and Ank2f02001 on the second chromosome resulting in the line UAS-Elk1-GFP/Cyo; Ank2f02001/TM6 (see appendix). To create homozygous Ank2 mutant larvae this line was crossed with a previously created stable line IGI-mCD8-RFP/Cyo; Ank2f00518/TM6. When the lines were crossed the resulting UAS-Elk1-GFP/IGI-mCD8-RFP; Ank2f02001/Ank2f00518 line could be confirmed with the lack of the TM6 phenotype, tubby larvae, and presence of both RFP and GFP under a confocal microscope.

RNAi Knockdowns

RNAi experiments used RNA hairpins to inactivate the gene that codes for the Dlg protein in order to knockdown Dlg and observe the resulting dmElk localization (Dietzl et al., 2007). This is done through the introduction of a short strand of RNA, cut by dicer, that binds with pre-existing mRNA creating a double stranded RNA that is then inhibited from translation or is destroyed (Fire et al., 1998). For these experiments, the Dicer2, mCD8-RFP; 22- Gal4, Elk1-GFP/TM6 line was crossed with Dlg RNAi (VDRC #109274).

Treatment of Crosses Prior to Imaging

Every 24 hours embryos were collected from the various crosses before being aged at 25ºC. All imaged larvae were 3-4 days old at the time images were taken. This time period allowed the larvae to be large enough to survive the mounting process but young enough that their exterior was still translucent enough to image through.

Confocal Microscopy Imaging

Larval Preparation and Set-Up

Non-tubby larvae were removed from their food caps and rinsed with distilled water before being screened to ensure both GFP and RFP were present. The positive larvae were placed dorsal side up on a microscope slide with dried agarose. The larvae were then covered with a glass cover slip held in place on the edges with translucent tape (Figure 2-1).

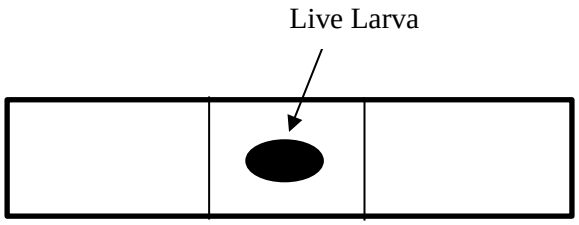

Figure 2-2: In-vivo imaging set-up.
This diagram illustrates the preparation of a live larva for imaging by placing it underneath a glass cover slip on a dry agarose covered slide.

Data Acquisition and Analysis

The mounted larvae were immediately imaged on a LSM 800 upright confocal microscope. GFP was excited using a 488 nm laser and RFP was excited through a 563 or 543 nm laser. The larvae where then imaged at a 63x 1.4 NA oil objective (T. Jegla et al., 2016).

All images were analyzed using ImageJ by drawing a line from the soma and down the axon to measure fluorescence levels at various points on the axon. The individual fluorescence intensities were then normalized as compared to the average bottom 25% and upper 5% intensity levels; the average, top and bottom values are represented in the localization graphs(T. Jegla et al., 2016).

Chapter 3

Localization of Voltage-Gated Ion Channels in the *Drosophila melanogaster* AIS

dmElk Localization

dmElk 5-2(2) Null Mutant Localization

In the *Drosophila melanogaster* ddaE sensory class I neurons, the dmElk channel was shown to localize in the assumed AIS. Two peaks of highest fluorescence, and therefore assumed channel concentration, were seen: one at 12.28µm and one at 27.23µm (Figure 3-1). The localization pattern closely matches the previously shown localization pattern for Ank2- a protein thought to border the AIS, Shal- another voltage-gated potassium channel, and other dmElk data (T. Jegla et al., 2016). This helps to confirm dmElks's presence in the putative AIS of *Drosophila*.

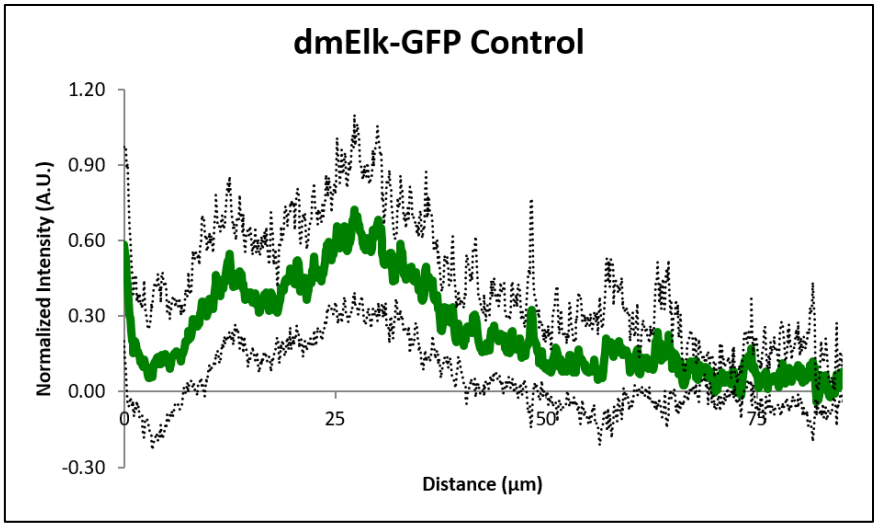

Figure 3-1 dmElk 5-2(2) Channel Control Localization.
This graph shows the average amount of fluorescence, representing the dmElk channel, in green and the standard deviation in black. The 0µm mark represents the soma and all other numbers are the distance down the axon from this point. (n=21)

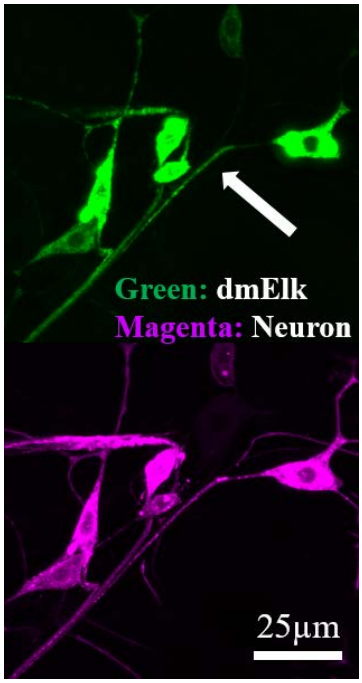

Figure 3-2: Example of dmElk 5-2(2) Channel Control Localization.
This image is a singular representative neuron created from the cross w;UAS-Elk-GFP x IGI-mCD8-RFP

dmElk Localization in an Ank2 Mutant Background

When the anchoring protein Ank2 was knocked out, little changed in the channel's localization. Two peaks of highest fluorescence were still seen at approximately the same location: one at 11.48µm and one at 30.21µm (Figure 3-3). However, the intensity of these points was decreased and the slope down from the second peak was shallower which could suggest a minimally more dispersed localization of the dmElk channel in the Ank2 mutant background.

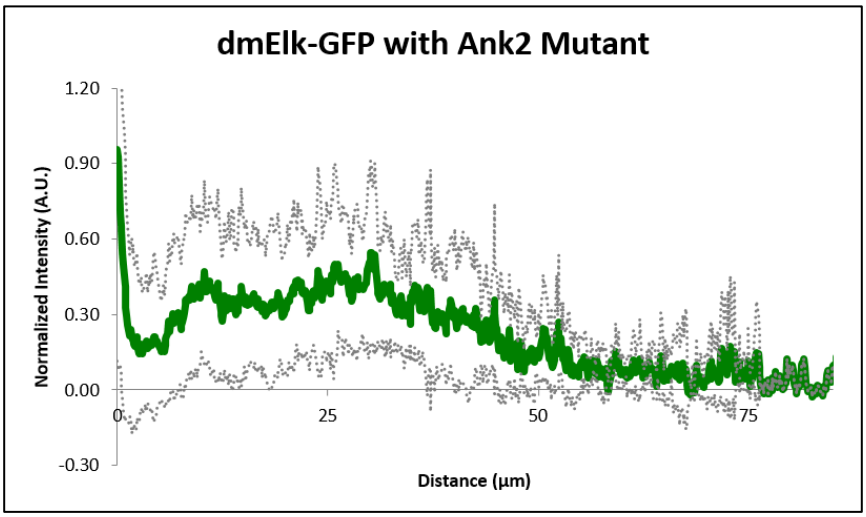

Figure 3-3 dmElk Channel Localization with Ank2 Mutant.
This graph shows the average amount of fluorescence, representing the dmElk channel, in green and the standard deviation in black. The 0µm mark represents the soma and all other numbers are the distance down the axon from this point. The anchoring protein Ank2 was genetically knocked out. (n=28)

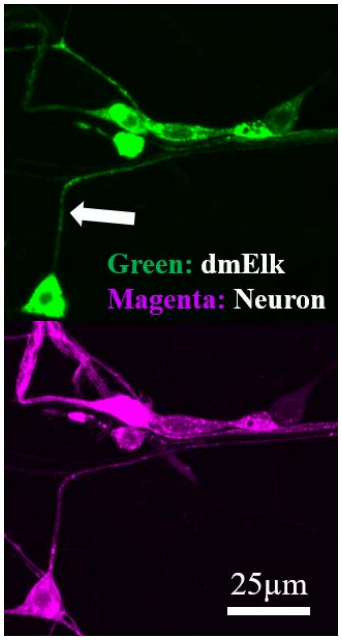

Figure 3-4: Example of dmElk Localization with Ank2 Mutant.
This image is a singular representative neuron created from the cross UAS-Elk-GFP/IGI-mCD8-RFP; Ank2fo2001/Ank2foo518

Dicer2, dmElk 3-2-2-1(3) Null Mutant Localization

When performing RNAi experiments, in order for the protein to be knocked down extra dicer2 must be added to cleave the dsRNA. In the case of dmElk this meant we need to use the gene on the third chromosome instead of the second chromosome, so we performed dmElk control data with this new third chromosome marker to determine its localization. Three peaks of highest fluorescence, and therefore assumed channel concentration, were seen: one at 25.08µm, 49.49µm and one at 67.84µm (Figure 3-5).

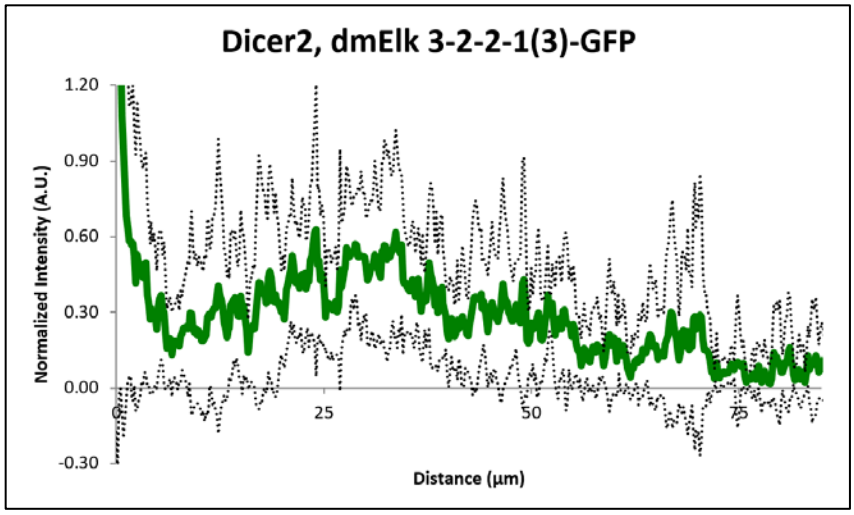

Figure 3-5 dmElk1 3-2-2-1(3) Channel Control Localization.
This graph shows the average amount of fluorescence, representing the dmElk channel, in green and the standard deviation in black. The 0µm mark represents the soma and all other numbers are the distance down the axon from this point. (n=8)

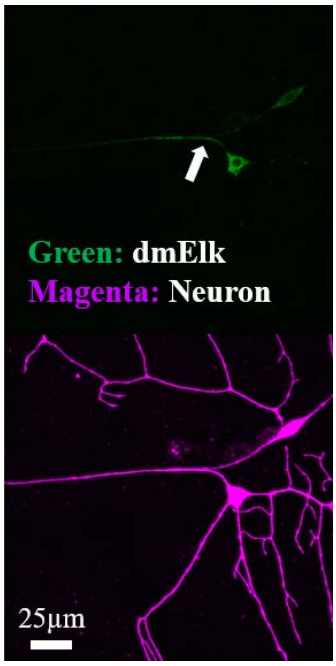

Figure 3-6 Example of dmElk 3-2-2-1(3) Channel Control Localization.
This image is a singular representative neuron created from the cross Dicer2, mCD8-RFP; 22- Gal4, Elk-GFP/TM6 x Dlg on II

dmELK Localization in Dlg RNAi Knock Down

Knocking down Dlg had the largest impact on the localization of the dmElk channel. The three distinct peak pattern disappeared and was replaced with an elevated plateau starting at 19.80µm and continuing to 48.28µm (Figure 3-7). This shift and extended period of fluorescence indicated a change in dmElk localization when the protein Dlg is reduced. This protein disruption may therefore have impacts on the AIS's ability to regulate subthreshold excitability.

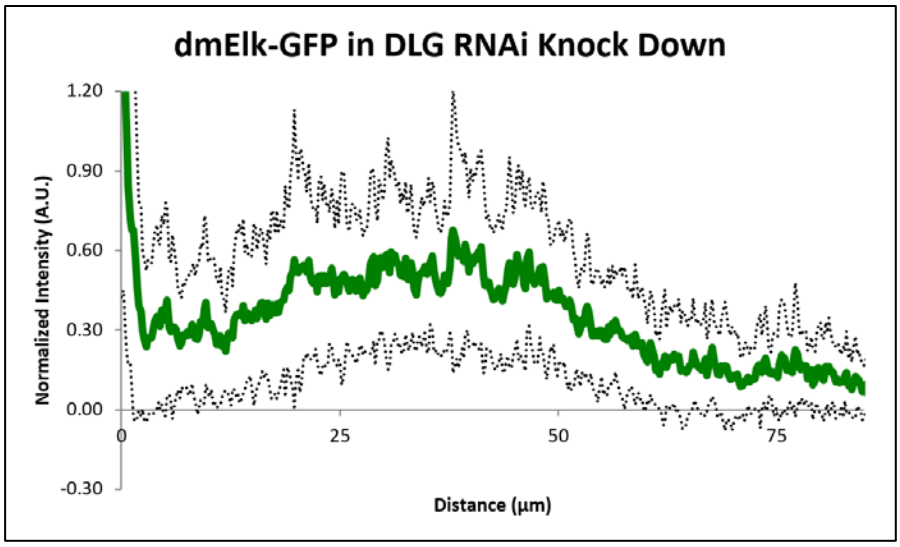

Figure 3-7: dmElk Channel Localization with discs large Knocked Down.
This graph shows the average amount of fluorescence, representing the dmElk channel, in green and the standard deviation in black. The 0µm mark represents the soma and all other numbers are the distance down the axon from this point. The anchoring protein discs large was genetically knocked out. (n=21)

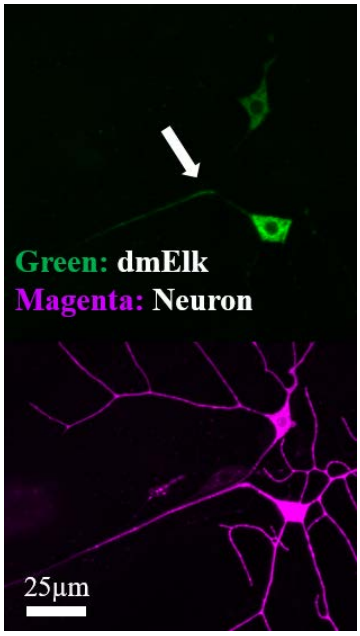

Figure 3-8: Example of dmElk Localization with discs large Knocked Down.
This image is a singular representative neuron created from the cross Dicer2, mCD8-RFP; 22- Gal4, Elk-GFP/TM6 x Dlg on II

Conclusion on dmElk Localization

DmElk channels were shown to localize in the putative AIS in *Drosophila* class I ddaE sensory neurons. These channels show little to no dependence on Ank2 in determining their localization. However, the anchoring protein Dlg may have a role in determining where in the AIS dmElk channels are found. At the same time it is important to note that the small sample size may have something to do with this apparent change in dmElk localization with Dlg knockdown. This localization pattern is the first indicator that dmElk channels may help in regulating subthreshold excitability like their vertebral ortholog, if dmElk gating properties also have similar hyperpolarized features.

Future dmElk Localization Directions

Since Dlg was shown to potentially impact the localization of dmElk channels future studies will include dmElk control bleaching experiments as well as bleaching experiments with Dlg knocked down to determine how this protein impacts the diffusion of the dmElk channel into the AIS. Since there was potentially a more diffuse pattern seen with Ank2 mutants, a bleaching experiment should also be done with the Ank2 mutant line. A future experiment should also look at β-spectrin as it has been shown to bind to giant-ankyrin as well as ion channels in vertebrates (Bennett & Lorenzo, 2013). We recently acquired a cleavable version of β-spectrin to start to look at this protein. As more genetic tools are developed, other anchoring proteins should be knocked out to determine how they may impact dmElk. These proteins could potentially include CAMs, actin, or microtubules; however, the other important functions of these proteins may make these proteins impossible to knock out in a viable manner (Jones & Svitkina, 2016). Other voltage-gated sodium, potassium, and calcium ion channels found in *Drosophila* should also be looked at

for their localization and dependence on anchoring proteins as they could also contribute to the generation and regulation of action potentials in the AIS.

Cacophony Channel Localization

Null Mutant Localization

The control localization data for the Cac channel showed a fluorescence intensity peak throughout the AIS, from 27.89µm to 44.07µm (Figure 3-9). This indicates that Cac channels are found in the putative AIS, not just solely in neuronal synapses, and may play a role in regulating action potential generation.

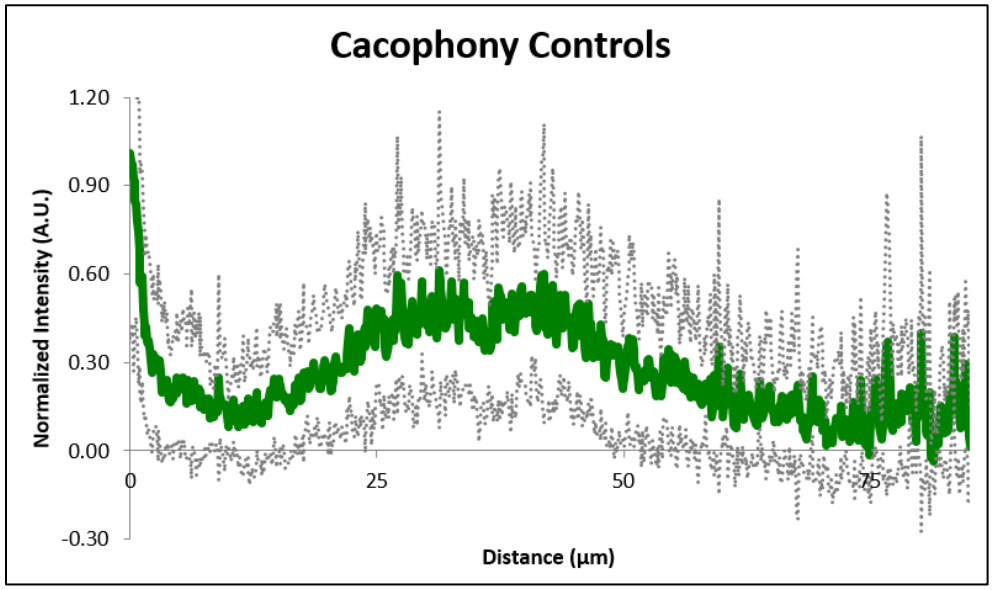

Figure 3-9: Cacophony channel Control Localization.
T*his graph shows the average amount of fluorescence, representing the Cac channel, in green and the standard deviation in black. The 0µm mark represents the soma and all other numbers are the distance down the axon from this point. (n=18)*

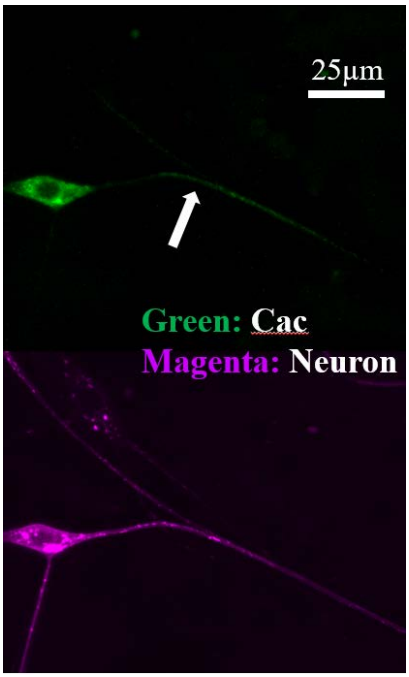

Figure 3-10: Example of Cacophony Channel Control Localization.
This image is a singular representative neuron created from the cross w;UAS-Cac1-eGFP422A x UAS-mCD8,mCherry

Future Directions For Cac Localization

Now that it is evident that Cac does localize in the putative AIS of *Drosophila* the next step involves determining which protein helps localize it. The first protein to be tried would be to test Dlg through RNAi due to evidence that this protein localizes Cac channels at synapses and therefore may play a similar role in the AIS (Astorga et al., 2016). Since the putative AIS is Ank2 dependent this would be the next anchoring protein to knock down to determine its impact on Cac localization.

Overview of Localization in the AIS

The presence of the Cac channel, in addition to the already known dmElk and Shal channels, gives more evidence towards the functionality of the putative AIS in regulating and initiating action potentials. The localization of these channels in control and knockout backgrounds are beginning to help illustrate the structure and borders of the *Drosophila melanogaster* putative AIS (Figure 3-5). While the below schematic suggests Dlg is localized in the putative AIS due to its impact on dmElk channels the actual localization data for the Dlg protein needs to be collected.

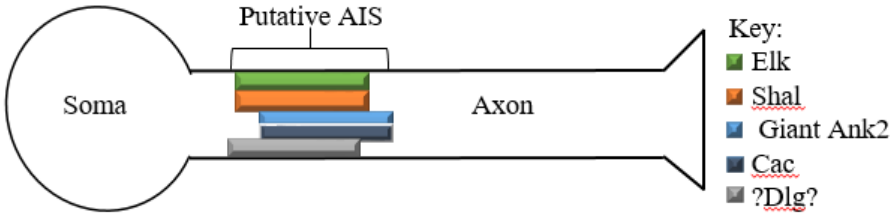

Figure 3-11: Diagram of the giant-Ankyrin AIS proposed distribution of channels and proteins.
This schematic includes Shal, dmElk, and Cac channels and Ank2 and Dlg anchoring proteins in the Drosophila ddaE sensory neuron. We hypothesized that Dlg is localized to the AIS due to dmElk localization dependence on Dlg but further studies will be needed to confirm this. The beginning of the segment is approximately 10µM from the soma.

Chapter 4

Techniques to Investigate dmElk and Elk1 Channel Properties

In order to look at the gating properties of the dmElk and Elk1 channels, RNA of dmElk and human Elk1 RNA was synthesized from a pOX DNA plasmid and expressed in *Xenopus laevis* oocytes before taking measurements using Two-Electrode Voltage (TEV) Clamp. During TEV measurements various solutions were used to observe a variety of characteristics of the channel.

Based on preliminary *Drosophila* Elk data presented below, we hypothesize that the channel has similar functionality in *Drosophila* and humans. This could suggest that if dmElk is localized in the putative AIS, as suggested above, the channel may help regulate subthreshold excitability in *Drosophila*, as in humans. Human Elk1 DNA was used to produce RNA instead of *Drosophila* DNA and RNA for the majority of experiments due to increased expression levels of the human version in comparison to *Drosophila* Elk. As previously described in the introduction to Elk1 channels, the Elk channel is a subfamily of the EAG family with highly conserved properties and functionality across evolution (Li, Martinson, et al., 2015). This suggests a high probability that we can relate the assumed *Drosophila* Elk and actual human Elk1 channels' functional data, but it should not be assumed that the channels are identical in all properties.

RNA and *Xenopus laevis* Oocyte Preparation and Injections

RNA Synthesis

The Elk1 DNA clone (GenBank accession number NM_144633) was previously amplified using RT-PCR and cloned into a pOX plasmid before the being confirmed via

sequencing (Li, Anishkin, et al., 2015). The pOX plasmid allowed the Elk1 gene to be placed between the 5' and 3' starting codons of Xenopus beta-globin, allowing stabilization of the mRNA which resulted in higher expression levels, making it a versatile tool for the integration of a variety of genes (T. Jegla & Salkoff, 1997).

The Elk1 expression vector was linearized via the high fidelity *Not*1 restriction enzyme, at a unique site in the plasmid. Then the T3 mMESSAGE mMACHINE kit (Invitrogen) was used to synthesize capped run-off cRNA transcripts. Lithium chloride was used to precipitate the transcripts followed by 70% Ethanol kept at -20ºC rinse, which removed cap analogs that can block ribosome function by 100 fold ("User Guide: mMESSAGE mMACHINE SP6 Transcription Kit," 2019). The pellets were air-dried before being resuspended into a 1:20 dilution of RNAse inhibitor (SUPERase-In; Invitrogen) in deionized water (>18 MΩ resistance) and stored at -80ºC to help preserve stability of the RNA. Transcript integrity was confirmed through gel electrophoresis on a 1.5% agarose gel and its concentration was determined to be 2697.0 ng/µL through the use of a nanodrop. dmElk RNA (Flybase ID: FBgn0011589) was prepared in the same manner as Elk1 and was resuspended at a concentration of 1-2 µg/µL.

Xenopus laevis **Oocyte Preparation**

Xenopus laevis ovaries were ordered from *Xenopus* 1. After the ovaries had been opened using thin-tipped forceps to increase the exposed surface area, the oocytes were enzymatically de-folliculated using 1mg/mL of Type II Collagenase (Sigma-Aldrich) in a pH 7.2 calcium-free ND98 solution (98mM NaCl, 2mM KCl, 3mM $CaCl_2$, 1mM $MgCl_2$, and 5mM HEPES). The collagenase broke down the membrane of the ovary, freeing the oocytes, and de-folliculated the individual oocytes. De-folliculated oocytes were then rinsed with the calcium-free ND98 solution before healthy oocytes were separated from damaged ones. The healthy oocytes were then stored

at 18ºC in a pH 7.2 ND98 culture solution composed of 98mM NaCl, 2mM KCl, 1mM MgCl2, 5mM HEPES, 2.5mM Na-pyruvate, 100 U/mL penicillin, and 100µg/mL streptomycin (Life Technologies).

RNA Injection of *Xenopus laevis* Oocytes

At the time of injection, different dilutions of the 2697.0 ng/µL Elk1 RNA were injected based on when recordings would take place to allow enough time for the RNA to be expressed into the Elk1 channels. All RNA volumes were taken from a 1:10 stock dilution and 50.6nL of the appropriate dilutions were injected into each oocyte by a Nanoject II injector (Drummond Scientific Company) at 46nL per second- the amount of Elk1 RNA injected ranged from 3.41ng to 13.65ng per oocyte (Table 4-1). 1µL of dmElk RNA in 4µL of deionized water was injected at a total concentration of 0.20ng/nl resulting in an injection of 50.6nL of 10.12-20.24ng of dmElk at a rate of 46nL per second. The various injected dilutions were empirically determined with the RNA batch to result in the largest current sizes possible without noise or potassium accumulation artifacts at the time of recordings. If the current size was too small the signal to noise ratio would be too high and if the currents were too large the rig would be unable to clamp (unpublished data). Large currents would result in large amounts of potassium efflux resulting in the accumulation of potassium in the extracellular fluid, which would change the driving force of potassium and cause the channel to depolarize, as is seen in large neuronal spikes during seizures (Jensen & Yaari, 1997). Based on observations of previous studies recordings we therefore aimed for currents between 5 and 20µA (Zhang et al., 2009).

In order to inject RNA, borosilicate glass micropipettes (Drummond) were first back-filled with nonpolar mineral oil via a spinal needle to create a liquid seal that does not mix with the polar RNA solution and prevents cross contamination between different RNA samples. The

micropipettes were pulled using a Model P-1000 Flaming/Brown Micropipette Puller (Sutter Instruments). After backfilling the micropipettes to create an interface between the RNA and the piston, the tip of the micropipette was broken off with forceps at a most distal point possible that still allowed the needle to be filled with RNA, resulting in ideal tip sizes of 10-30 microns ("Nanoject II Auto-Nanoliter Injector," 2019). A fine tip was used to cause minimum damage and scarring to the oocytes during the injection process, allowing them to survive longer. Once the tip was broken, the needle was lowered into a 5µL droplet of an RNA dilution and front filled using a negative pressure created by the retraction of the piston. At this point the needle was prepped for injection and the oocytes were placed onto a notched petri dish, to keep them still. The needle then punctured one oocyte at a time and 50.6nL of the predetermined RNA concentrations were injected into the oocyte at a rate of 46nL/second. The injected oocytes were then incubated at 18ºC for two to five days to allow for function expression of the dmElk or Elk1 channels in the oocyte.

Table 4-1: The Varieties of RNA Injection Concentrations.
Based on the number of days after injections that recordings would be taken on oocytes determined the concentration of Elk1 RNA injection into the Xenopus oocytes. The undiluted concentration for the Elk1 RNA was 2697.0 ng/µL. Each injection was a volume of 50.6nL at a rate of 46nL/second.

Days Post-Injection Till Recording Session	**RNA Volume**	**Deionized Water Volume**	**Approximate Final RNA Concentration**	**Amount of RNA injected into each oocyte**
2-3	5uL of a 1:10 dilution	0uL	269.7ng/µL	13.65ng
3-4	2 uL of a 1:10 dilution	3uL	107.88ng/µL	5.46ng
4+	1uL of a 1:10 dilution	4uL	53.94ng/µL	2.73ng

Solution Preparations

Various solutions were prepared in order to analyze the effect of various proteins and ions in the Elk1 channels. All solutions were constructed from a control pH 7.5 solution. The

control solution's base was deionized water (>18 MΩ resistance). The makeup of the control solution included 98mM NaOH, 2mM NaCl, 5mM KCl, 1mM CaCl and 5mM HEPES. When testing the effects of zinc and heme, this standard solution were supplemented with these molecules. For dmElk control pH6, pH7, and pH8 solutions were used. They all included 98mM NaOH, 2mM NaCl, 2.5mM KCl, 1mM CaCl and 5mM HEPES.

All solutions that included zinc or heme added the additional component to the previously mentioned control pH 7.5 solution just prior to TEV recordings.

For zinc, a 300μM zinc recording solution was prepared using a stock of 1M zinc solution. This solution was placed in perfusion tubes and flowed over the oocyte during recording sessions after impalement in the control pH 7.5 solution.

Heme (Sigma-Aldrich) solutions were made from a stock of 10mM heme (6.5mg of heme in 1mL of water and 20uL of 1M NaOH). The recording solutions included 300nM heme, 1μM heme, 3μM heme, and 10μM heme. For heme experiments, oocytes were soaked in one of these solutions 5-10 minutes prior to being placed on the rig for recordings. This allowed the heme to bind and take effect. Recordings were then taken in a control pH 7.5 solution. Doing a presoak in heme was sufficient to observe the effect of the molecule on the channel as it has been observed in our lab that the heme does not wash off within the time frame of the recording sessions (unpublished data).

When combined heme and zinc experiments were performed, the oocytes were first presoaked for 5-10 minutes in a heme solution and placed on the rig, then they were impaled in control pH 7.5 solution, and finally the 300μM zinc solution was flowed over the oocyte during recordings. The reasoning behind presoak with heme rather than putting both heme and zinc in one solution was to prevent crystallization of the molecules. Crystallization could clog pipping, alter concentrations, and alter the rate of flow for various solutions.

Between all solution changes, a ramp protocol was used to ensure that the new solution had taken full effect prior to the recording of a GV. Impalements were done in the pH 7.5 control solution to ensure no zinc or heme entered the oocyte.

Table 4-2: Solution Preparations.
This table illustrates the solutions used for each part of the experiment including controls, Heme controls, Zinc controls, and Heme with Zinc experiments.

Main Solution	Heme Concentration: 5-10 minute Presoak	Zinc Solution
pH 7.5	0	0
pH 7.5	0	300µM
pH 7.5	300nM	0
pH 7.5	1µM	0
pH 7.5	3µM	0
pH 7.5	10µM	0
pH 7.5	300nM	300µM
pH 7.5	1µM	300µM
pH 7.5	3µM	300µM
pH 7.5	10µM	300µM

Electrophysiology

Data Acquisition

Currents in mature *Xenopus* oocytes expressing *Drosophila* Elk or human Elk1 were recorded using two-electrode voltage clamp (TEVC). TEVC recordings were done by clamping the oocytes using a Dagan CA-1B amplifier (Molecular Devices. All collected data was acquired and analyzed using pClamp 10 suite (Molecular Devices). Data was sampled at a rate of 10kHz and filtered at a low-pass rate of 2-5kHz.

Glass electrodes (0.4-1 MΩ) were pulled using a Model P-1000 Flaming/Brown Micropipette Puller (Sutter Instruments). Electrodes were backfilled with 3M KCl. 3M KCl was chosen as the least resistant compatible solution to the interior of the oocyte in case there was minor leakage into the cell. Potassium was used instead of sodium as sodium inside of the oocyte

is toxic and instead of cesium since cesium blocks the Elk channels. Due to the sharp and small electrode tip we did not need to account for the molarity of the inner fluid of the oocyte. Bath electrodes were placed in a 1M NaCl bath and connected to the circuitry through a 1M NaCl-agarose bridge. The agarose bridge prevented offset of bath electrodes due to major changes in the ion flow upon the perfusion of various solutions through the system and maintained the natural concentration gradient.

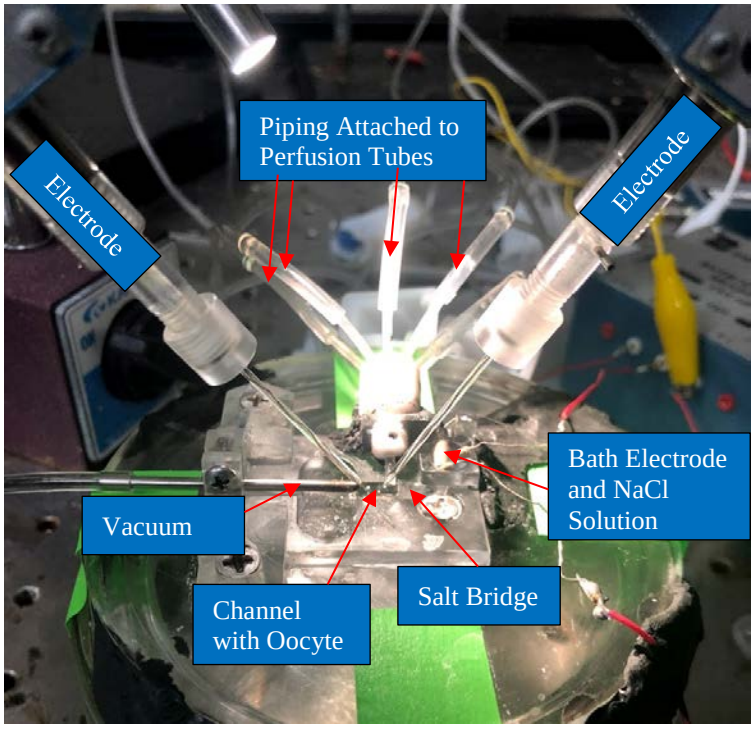

Figure 4-1: TEVC Set Up.
This image illustrates the proper set up of TEVC for oocyte recordings.

The oocyte sat, slightly elevated from the bottom of the container in a channel. This channel was filled with the current solution being flowed over the oocyte from the perfusion tubes allowing components of the solution to interact with the dmElk or Elk1 channels expressed on the oocyte membrane. Excess solution was then removed from the system through a continuous vacuum (Figure 4-1).

Data Analysis

Voltage –activation (GV) curves were measured at the isochronal tail currents of -40mV for Elk1 and at 0mV for *Drosophila* Elk channels to determine channel activation properties for each preceding voltage change. Raw data for each oocyte was used to create individualized Boltzmann curves using the equation $G(V) = \left[\frac{A1-A2}{1+e^{(V-V_{50})/dx}}\right] + A2$ where G is the conductance at voltage (V), A1 is the lower bound, A2 is the upper bound, V_{50} is the half-maximal activation voltage, and *dx* is the slope factor. All data points (V(x)) were normalized using upper and lower bounds with the equation $\frac{(V(x)-A1)}{(A2-A1)}$ and are presented as normalized V_{50} and slope factor averages ± Standard Error Mean and are shown with a simulated Boltzmann curve. Normalizing the data allowed us to combine each individual oocyte with equal weight into the plotted averages while the simulated Boltzmann curve is based on the average V_{50} and slope factors determined by individual raw fits, within the normalized limits.

Chapter 5

dmELK and Elk1 Channel Properties

Background on Channel Gating

As previously mentioned, Elk1 channels are voltage-gated potassium channels. Under normal conditions the channels are closed at a hyperpolarized resting membrane potential and open when a specific depolarized voltage is reached, allowing the efflux of potassium ions. The mechanisms controlling the gating of the ion channel are known to be determined by voltage sensors which detect whether or not the environment is hyperpolarized or depolarized. It has been suggested that Elk1 channels activate in a pH 7.5 solution at hyperpolarized levels positive of -90mV, where about half of the channels are open at -62mV, in a similar fashion to the Shaker channels discussed above (Zou et al., 2003). Elk1 is believed to help regulate subthreshold excitability, so it would be expected that the activation range of the channel overlaps the typical resting potentials and threshold voltages (Zhang et al., 2010).

These channels are made of four subunits each of which are made of six transmembrane units (Figure 5-1A) in a similar fashion to the related Eag1 channels (Bernsteiner, Brundl, & Stary-Weinzinger, 2017; Whicher & MacKinnon, 2016). The first four transmembrane units are the voltage sensor and the last two are related to pore construction of the channel (Figure 5-1B). Related Shaker channels have shown evidence of voltage-sensing residues on the S4 segment which are critical to activating the sensor (Liman, Hess, Weaver, & Koren, 1991). These positive residues, also referred to as gating charges, interact with the negative charges found in extracellular and intracellular charge clusters on the S2 and S3 segments allowing the S4 segment to shift out of the way of the pore (Liman et al., 1991). The residues are found at an aqueous

cavity on the exterior of the voltage sensor which partly helps to indicate how the gating mechanism can be regulated by pH changes, divalent ions, and heme, as discussed below. In order for Shaker and related channels to be open all four voltage sensors must be activated, causing them to physically shift with the linker to move out of the way of the pore and allow potassium ions to pass through (Figure 5-1C) (Kalstrup & Blunck, 2018).

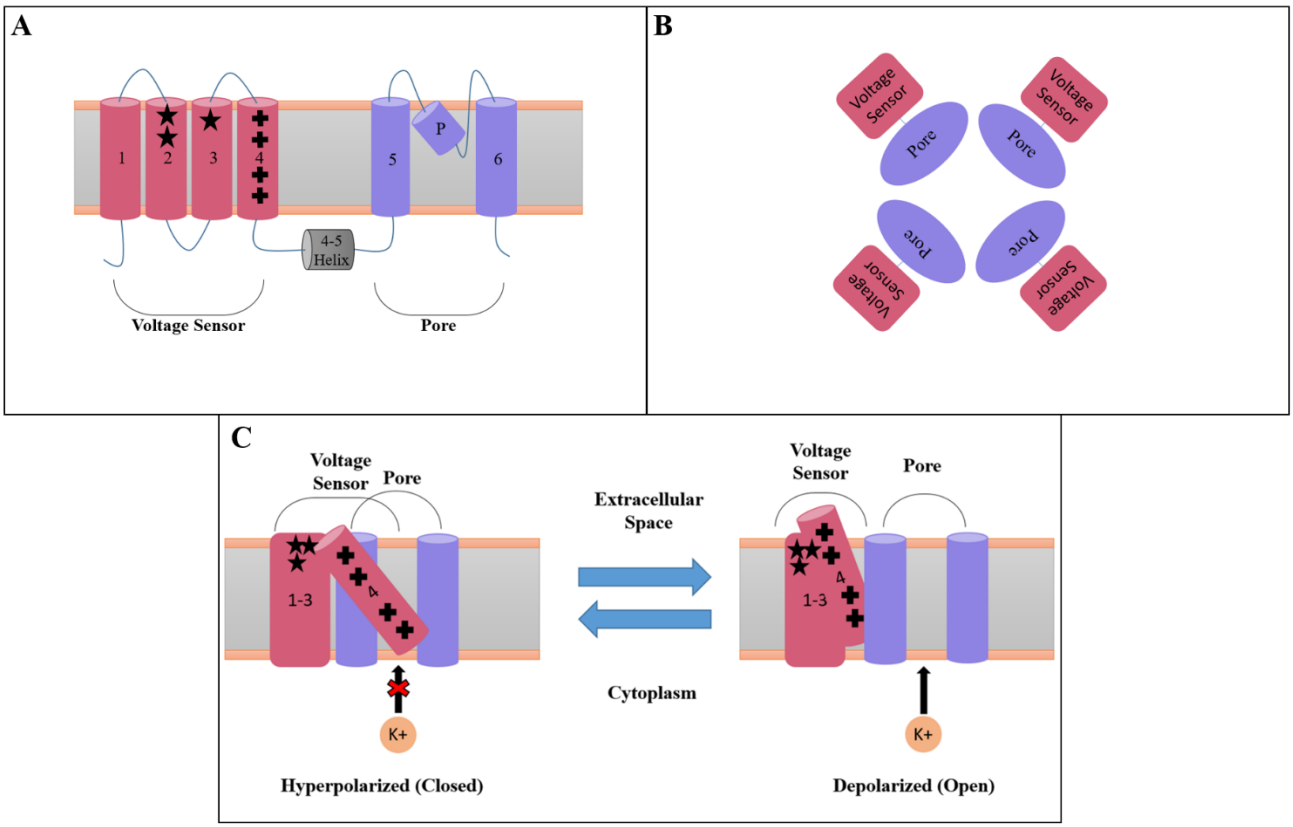

Figure 5-1: Diagram of Voltage-Gated Elk1 Channel Composition.
This diagram illustrates how voltage gated ion channels are composed of 6 transmembrane units each with specific functions (A) that make up four subunits (B). The final schematic represents the way that the S4 region of the voltage sensor moves out of the way of the pore as the basic gating charges (+) are stabilized by the negative charges of the extracellular charge clusters (star). The movement of S4 allows ions to flow through once all four voltage sensors go through this change (C). When discussing the interaction of zinc and heme with the channel we are talking about the extracellular charge clusters on the S2 and S3 transmembrane proteins (stars).

The current gating properties of dmElk have not been elucidated. We expect that the channel will activated at hyperpolarized voltages due to conserved properties across voltage-gated potassium channels and due to the fact that it localizes within the putative AIS of

Drosophila. We will also be looking at pH changes for dmElk to see if this channel appears to have the same or similar regulation of gating properties as Elk1. The regulation of gating properties of Elk1 will further be explored to determine how heme and zinc, which have been observed to impact the gating of Elk1 channels, may participate in regulation of the channel either through the same or different extracellular charge clusters of the S2 and S4 segments.

pH Regulation of Voltage-Gated Channels

It has been suggested that the regulation of gating in voltage-gated potassium ion channels has to do with the protonation state of extracellular S2 and S3 acidic residues (Kazmierczak et al., 2013; Silverman, Tang, Mock, Huh, & Papazian, 2000; Zhang et al., 2009). More specifically, it has been shown that protons bind to these acidic residues causing them to become neutralized; therefore, preventing the stabilization of the S4 gating charges and the subsequent movement of the S4 segment out of the way of the Elk1 channel pore (Kazmierczak et al., 2013). This protonation block explains why channels exhibit pH sensitivity and have been seen to open at more hyperpolarized voltages in basic pH solutions, as less protons are present to block the channel by protonating the S2 and S3 charges (Kazmierczak et al., 2013). Neutralization of these channels through mutations has also show an inhibition of channel activation as this is an artificial way to protonate the acidic residues leading to the prevention of S4 movement and stabilization (Kazmierczak et al., 2013; Silverman et al., 2000; Zhang et al., 2009).

Divalent Regulation of Voltage-Gated Channels

Divalents, as previously mentioned, have been shown to directly compete with protons for binding spots on the extracellular acidic residues of EAG family channels, allowing divalents to be used as an indicator of channel sensitivity to protons (Kazmierczak et al., 2013; Silverman, Bannister, & Papazian, 2004; Silverman, Roux, & Papazian, 2003). This competitive binding makes sense as both protons and divalents will want to bind with the negative charges found in the extracellular residues and increased pH seems to sensitize Elk1 channels to divalents as less proton competition is present (Kazmierczak et al., 2013; Silverman et al., 2000).

While many different divalents can play a role in channel blocking, magnesium has been shown to act as a block in the aqueous cleft of Eag channels (Silverman et al., 2000). While in this aqueous cleft, magnesium has been shown to bind with the S2 and S3 extracellular charges and acts as an indirect inhibitor of the S4 gating charges on the other side of the cleft (Silverman et al., 2000). Although closely related, the Elk1 channel has a different charge configuration than Eag channels, resulting in the divalent ion zinc blocking the channel instead of magnesium (Zhang et al., 2009). Based on previous data showing the sensitivity of Elk1 channels to zinc, a 300μM concentration of zinc was chosen for these experiments to ensure an effect could be seen when zinc and heme were both applied, whether there was a right or left shift of the GV (Zhang et al., 2009). This thesis looks at zinc alone to see its effects on Elk1 gating and then combined with heme to see whether heme impacts zinc's effect or if zinc impacts heme's effect, depending on which molecule is a potentiator could help clarify a potential mechanism for the regulation of gating via heme and zinc. Their interaction could also shed light onto whether or not there is one or multiple binding sites that are involved in protonation regulation.

Heme Regulation of Voltage-Gated Channels

Our lab has previously observed that heme is a strong modulator of the gating properties of voltage-gated channels (unpublished data). We have seen that for the Elk1 channel heme causes a left-shift in the voltage gating, allowing the channel to open at more hyperpolarized voltages (Figure 5-2). However, the mechanism behind this shift is currently unknown and is begun to be explored within the context of this thesis.

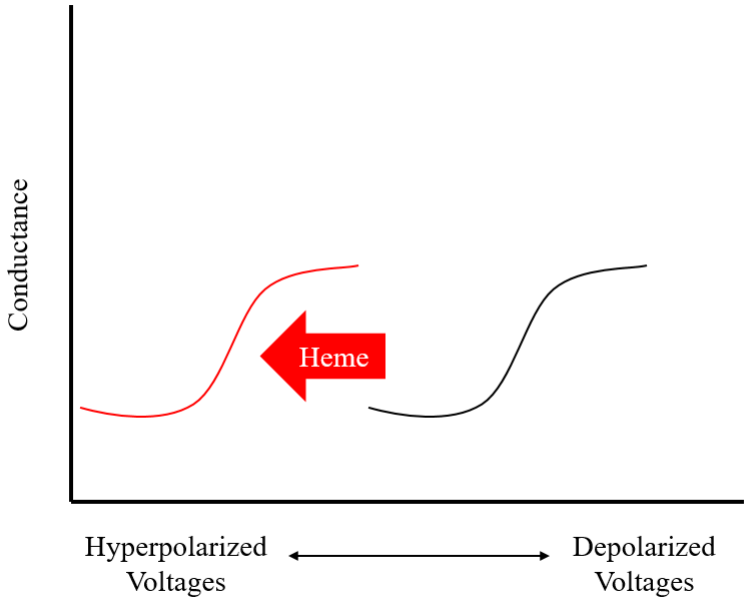

Figure 5-2: Schematic of the Predicted Effect of Heme on Channel Gating.
This diagram illustrates the left shift of the activation of channels upon the addition of Heme

Previous studies, as discussed, have determined that Elk1 channels are highly sensitive to pH due to competitive inhibition by protons (Kazmierczak et al., 2013). Here we tested the hypothesis that heme, a term for a protoporphyrin ring containing iron, activates Elk1 channels by deprotonating (or increasing the net negative charge of) the external charge cluster. If so, then it should activate the channel at hyperpolarized voltages and also sensitize the channel to zinc block. Our hypothesis is that zinc and heme combined would result in a far right shift due to

deprotonation by heme making it easier for zinc to bind to the channel and block it more effectively.

More specific terminology is sometimes used for heme. Hemin which is dissolved during solution preparation in this experiment has a chloride ion attached. The dissolved product is hematin, which has a hydroxyl anion. Upon interaction with the channel the hydroxyl can stay on or be removed. Since the exact form is unknown, we will use the generic term heme when referring to this molecule. In the case of this thesis, the molecule was used to see how it impacted gating and combined with zinc how it impacted gating, the resulting interaction of which could lead to a better understanding of how an extracellular bind could impact intercellular gating mechanisms in voltage-gated potassium channels.

dmElk Functional Properties

dmElk Channel Gating Properties

The following shows preliminary data for dmElk channels and illustrates a similarity in dmElk and Elk1 channels' kinetics (Fig 5-3). Even though it is seen that dmElk activates at a more depolarized voltage that Elk1 this channel still significantly activates at subthreshold voltages and around threshold voltages. This subthreshold activation of dmElk channels is important because it shows evidence that there is a high chance the dmElk and Elk1 are performing the same tasks in their respective AIS regions. Similarities like this allow the channels to be used as models for one another to overcome experimental obstacles in using one or the other channel. Obtaining data for dmElk is difficult due to its low expression levels in oocytes. It is critical to note that a more hyperpolarized activation is seen with increased pH as this reflects the idea of proton blocking regulation as seen in Elk1 channels (Kazmierczak et al., 2013). While pH

6 data was collected it made current sizes so small it was impossible to extract a GV, hinting that the protons were blocking most of the channels from opening. This evidence of a proton block in dmElk channels provides reason to believe that dmElk and Elk1 channel gating could be regulated in a similar fashion.

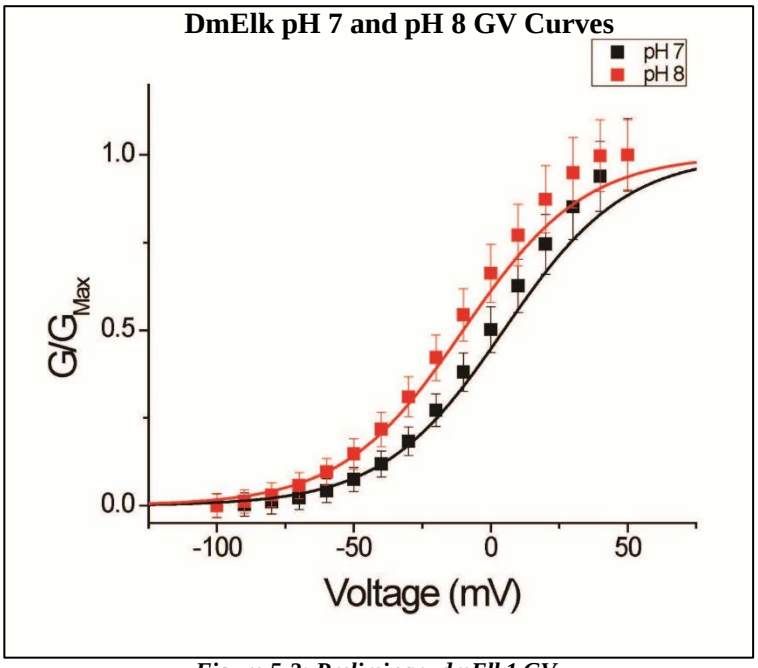

Figure 5-3: Preliminary dmElk1 GV.
This graph illustrates the conductance of the dmElk channel's tail currents at various voltages in both pH 7.0 and pH 8.0 to illustrate the similarities of drosophila and human Elk1..

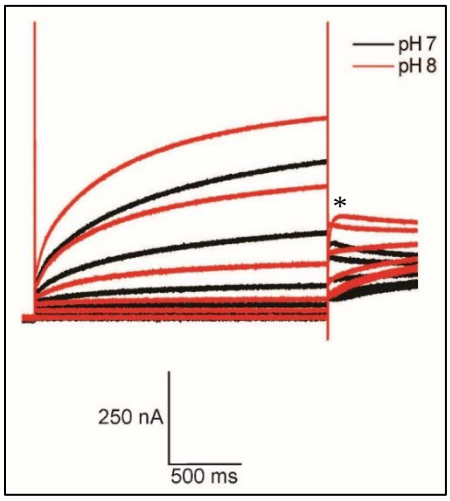

Figure 5-4: Example Trace of dmElk recordings.
These traces illustrate the raw data obtained during TEVC readings. The "" represents the location at which values were taken for the GV.*

dmElk Future Directions

At this point is hard to continue studies with dmElk due to its low expression levels. If we are able to discover a way to increase dmElk mRNA expression in oocytes then we will want to perform heme and zinc studies with this channel to help determine if the two channel types are have gating regulated in the same way. It is possible increasing mRNA injection concentrations may aide in higher dmElk channel expression; however, we have currently seen that this mostly leads to increased lethality of oocytes prior to recording periods, as is common in low expressing RNA (unpublished data). One possibility for increased expression of dmElk may be the process of polyadenylation, which has been shown to increase translational efficiency of mRNA in Xenopus oocytes as the dmElk used was capped but did not have a poly(A) tail (Drummond, Armstrong, & Colman, 1985). However, preliminary data in our lab showed that this was not effective. One solution could be using *Drosophila* trafficking genes to increase trafficking of the channel to the surface membrane, but this is a large effort for relatively low payoff.

Elk1 Functional Properties

When looking at the gating properties of channels it is common practice to compose GV curves. These graphs look at the conductance of the channel versus the voltage at that point. A higher conductance value correlates with more channels being open. The standard in the field is to look at the V_{50} on GV curves. This is the voltage at which half of all ion channels expressed in the cell are considered open.

Divalent Effect of Elk1 Gating

The V_{50} for Elk1 channels in a pH 7.5 control solution was calculated to be -67.01mV (Figure 5-5). The introduction of a 300µM zinc solution during TEV measurements caused a large right shift of approximately 42mV in the GV curve, in line with previous research observed shifts, for Elk1 channels, as compared to control data, resulting in a V_{50} of -24.99 (Figure 5-2). This suggests that the zinc divalent blocked the Elk1 voltage sensor making it harder for the channel to open. The channel only opened at higher depolarized voltages due to the increased positive charges pushing the zinc off of the sensor, allowing the channel to open and allow the conductance of potassium through the channel.

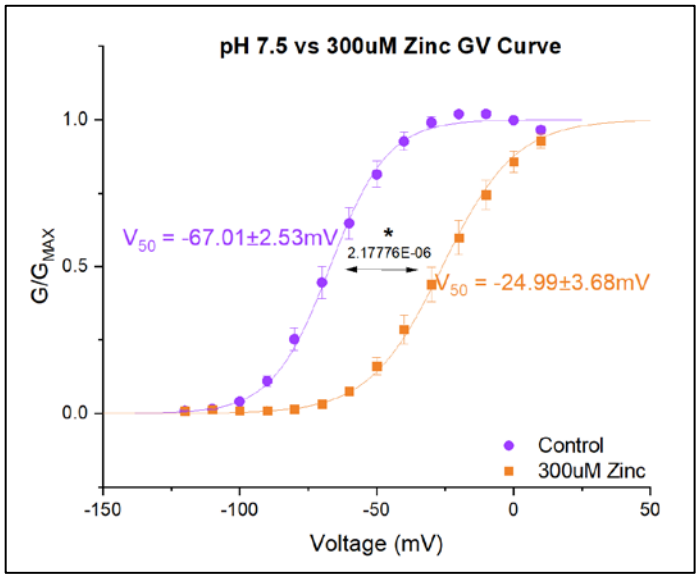

Figure 5-5: pH 7.5 vs 300uM Zinc Elk1 GV.
This graph illustrates the conductance of the channels' tail currents at various voltages under control and 300µM zinc. The V50 for pH 7.5 is marked as -67.01±2.53mV (n=7). The V50 for 300µM zinc is marked as -25.99±3.68mV (n=7). A "" indicates a value of $p < 0.05$ between control and zinc conditions.*

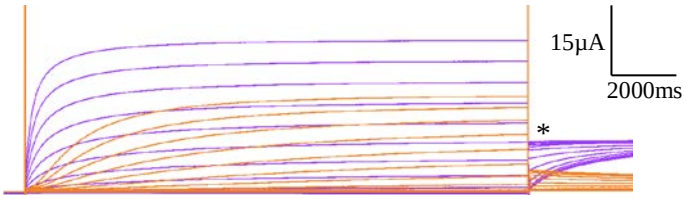

Figure 5-6: Example Trace of Elk1 recordings with and without zinc.
These traces illustrate the raw data obtained during TEVC readings. The "" represents the location at which values were taken for the GV. The purple curve represents pH 7.5 control data while the orange curve represents the 300µM zinc data.*

Heme Effect on Elk1 Gating

The introduction of heme to the Elk1 channels caused a left shift of the GV curve resulting in V_{50}s between -69.90mV and -116.29mv (Figure 5-7). Concentrations of 300nM, 1µM, 3µM, and 10µM were tested with progressively larger left shifts seen for each. This shift, reflected an easier opening of Elk1 channels at lower voltages, suggesting that heme is deprotonating each of the four voltage sensors, causing them to shift into the open state. The continued shift in the GV suggests that at 10µM heme has not reached its maximum effect on gating. This also suggests that in order for heme to open ion channels at more hyperpolarized voltages, all four voltage sensors must be bound with and stabilized by heme.

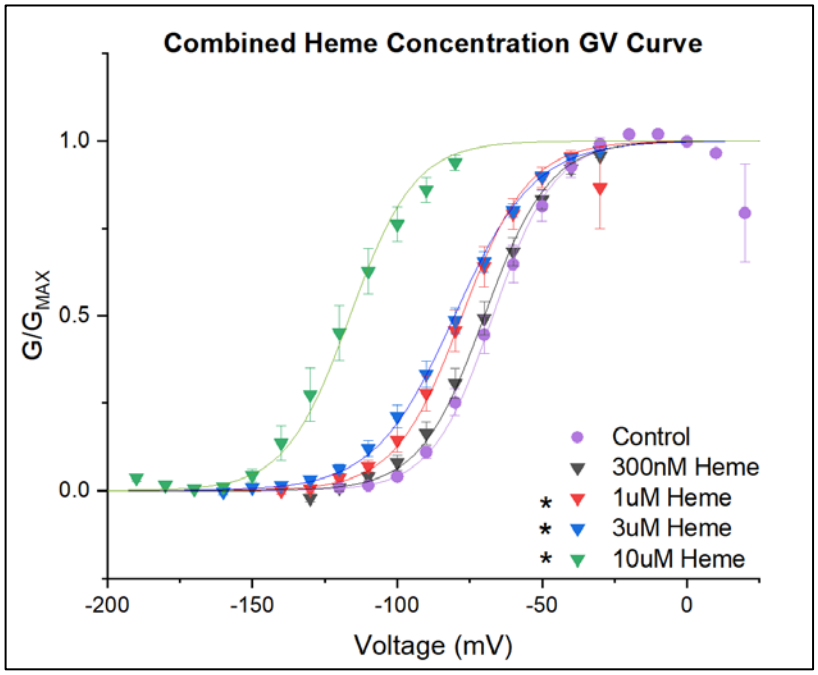

Figure 5-7: pH 7.5 Elk1 Heme control GV.
This graph illustrates the conductance of the channels' tail currents at various voltages with the addition of Heme at different concentrations: (300nM Heme (V50= -69.90±2.43mV, n=16, p= 0.421751323),1µM Heme (V50= -77.64±3.22mV, n=9, p=0.021101564) , 3µM Heme (V50= -80.25±2.23mV, n=13, p=0.001412304), 10µM Heme (V50= -116.29±3.95mV, n=9, p= 1.02349E-07). A "" indicates a value of p < 0.05.*

Combined Divalent and Heme Effect on Elk1 Gating

After a presoak in a heme solution and introduction of the 300µM zinc solution to the oocyte, Elk1 channels exhibited a right shift of the GV curve greater than when just zinc was present, with a V_{50} between -7.35mV and -5.62mV (Figure 5-8). This significant shift from baseline illustrates that heme sensitizes the channel to zinc allowing zinc to more easily bind to the Elk1 channel and leading to a decreased probability of the Elk1 channels opening. This could potentially be caused by deprotonation through heme. All four concentrations of heme- 300nM, 1µM, 3µM, and 10µM- with zinc showed final values within less than 3mV of each other, all of which were statistically identical. This lack of change between the heme concentrations suggests that at 300µM zinc all heme concentrations maxed out the effect of zinc. However, in order to

confirm this we would need to establish the maximal zinc effect without any heme involved. We also would need to look at lower zinc concentrations to see how much of an effect heme can have at lower concentrations when zinc is not at its maximal effect.

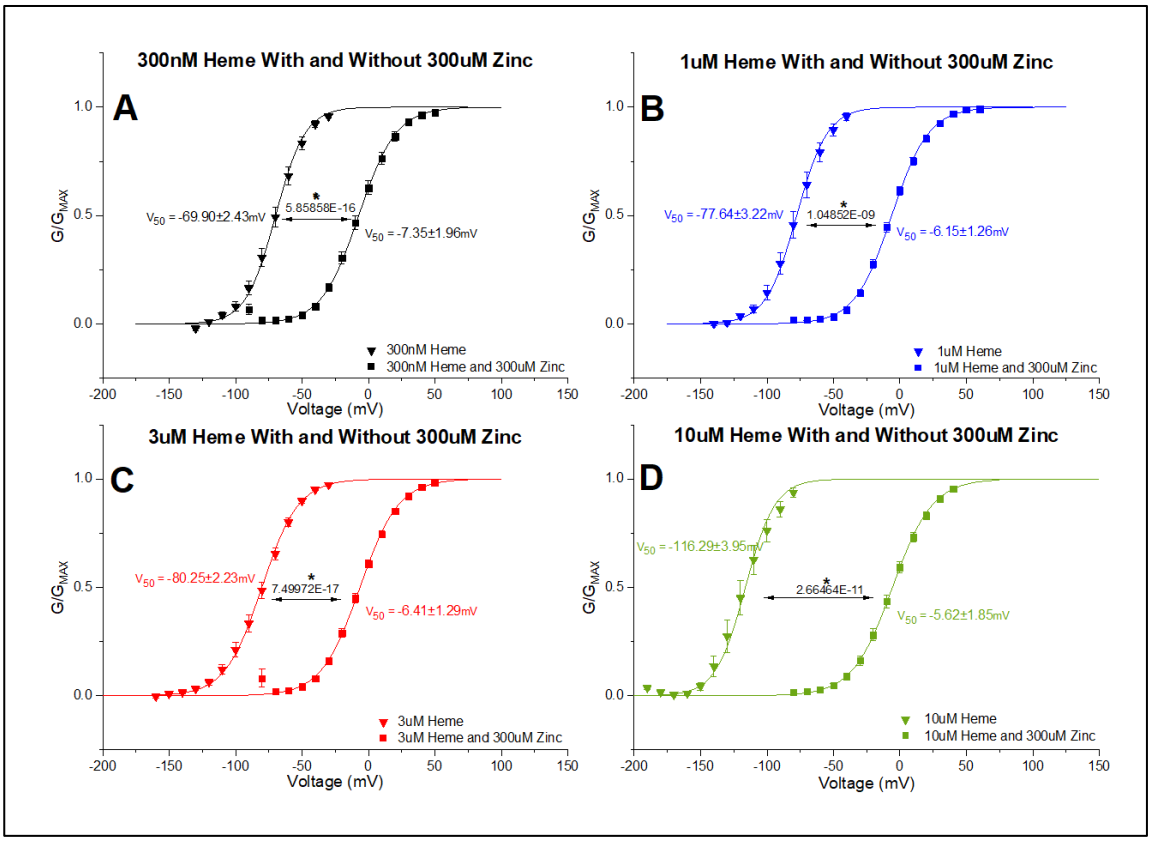

Figure 5-8: pH 7.5 Elk1 Heme with Zinc Experiments GV.
This graph illustrates the conductance of the channels' tail currents at various voltages with the addition of Heme at different concentrations and Zinc at 300µM: (A) 300nM Heme and 300µM Zinc, (B) 1µM Heme and 300µM Zinc, (C) 3µM Heme and 300µM Zinc, (D) 10µM Heme and 300µM Zinc. A "" indicates a value of $p < 0.05$ between the heme and heme with zinc conditions.*

These results beg the question of in what way heme and zinc are interacting to control channel gating and whether or not they share the same binding site. Our hypothesis is that there are two allosteric sites, one for heme and one for zinc, allowing the heme to potentiate the effects of zinc on Elk1 gating. If the two molecules were competitive we would expect to see that when heme is applied more zinc would be needed to get the normal zinc effect or vice versa, neither of

which is seen in these results. On the other hand, non-competitive antagonists would not impact the effect of each other. Therefore, the strongest explanation is that heme is an allosteric potentiator, potentially through the deprotonation of charges effectively removing the protons that zinc normally competes with directly.

Further evidence that heme is actually sensitizing the Elk1 channel to zinc's blocking effects is seen by comparing the delta V_{50}s of each heme concentration when zinc is and is not present (Figure 5-9). It was observed that there was a significant increase in delta V_{50}s for at least all heme concentrations tested including and above 1µM heme. This suggests that heme potentiation sensitized the channel to zinc causing a right shift in V_{50}s, further illustrating that there is most likely two separate amino acid clusters being impacted by heme and zinc.

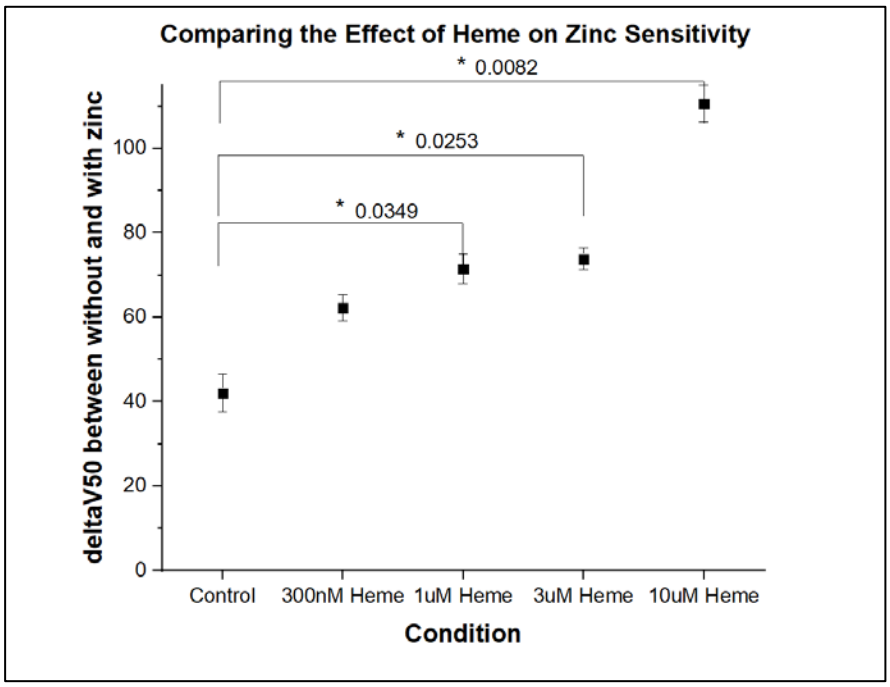

Figure 5-9: Comparing the Effect of Heme on Zinc Sensitivity.
This scatterplot graphs the delta V_{50} between conditions with and without zinc for each heme concentration. Each V_{50} was compared to the control solution with and without zinc to see if heme was sensitizing the channel to zinc. A "" represents a p-value of less than 0.05. deltaV_{50}s with and without zinc were as follows: Control (42.02±4.47mV), 300nM Heme (62.25±3.12mV), 1µM Heme (71.49±3.46mV), 3µM Heme (73.84±2.58 mV), and 10µM Heme (110.667±4.36mV)*

Summary of Elk1 Gating Data

The following summarizes the Elk1 data presented within this section (Table 5-1). It reemphasizes that we saw a hyperpolarized activation of Elk1 channels, which shifted to the left upon the addition of heme, to the right with zinc, and was even farther shifted to the right with both heme and zinc due to heme's potentiation effect on zinc binding.

Table 5-1: Overview of Elk1 Functional Data

This table illustrates the V_{50} average, where half of the channels are open, the slope averages, activation rate, and the number of oocytes used for each average of the 10 conditions previously shown in the chapter 5 figures.

Condition (all pH 7.5)	V_{50} Average (mV)	Slope Average (G/G_{MAX}/mV)	Number of Oocytes in Averages	P-Value Compared to Control
Control	-67.01±2.53	10.54±0.46	7	--
300nM Zinc	-24.99±3.68	13.37±0.47	7	*2.17776E-06
300nM Heme	-69.90±2.43	11.20±0.34	16	0.421751323
1µM Heme	-77.64±3.22	11.60±0.39	9	*0.021101564
3µM Heme	-80.25±2.23	13.82±0.46	13	*0.001412304
10 µM Heme	-116.287 ±3.95	12.57±0.71	13	*1.02349E-07
300nM Heme and 300nM Zinc	-7.35±1.96	14.10±0.45	9	*2.73743E-10
1µM Heme and 300nM Zinc	-6.15±1.26	13.94±0.58	6	*7.34652E-09
3µM Heme and 300nM Zinc	-6.41±1.29	14.53±0.22	10	*4.33469E-09
10 µM Heme and 300nM Zinc	-5.62±1.85	15.07±0.42	8	*4.10642E-10

Future Directions

Due to a lack of differences in gating effects between the four heme concentrations at 300µM zinc, the next step would aim to figure out at what levels zinc has its maximal effect. To do this, we would look at higher zinc concentrations, such as 1mM, without heme. We would expect that this maximal effect would be around -6mV as that is approximately where the combined heme and zinc effects stabilized in this study. Another thorough follow-up study would involve looking at lower concentrations of zinc, including 100µM and 10µM, at the various heme

concentrations previously mentioned. This would allow us to see the differences in effect heme combined with zinc can have when it is not at its maximal effect. This would allow us to make a dose-response curve and further understand to what extent heme is potentiating zinc.

Another future direction that is starting to be worked on in our lab is using amino acid mutations on the voltage sensors to test gating regulation. These mutated channels can be observed under heme, zinc, and heme and zinc conditions in an attempt to better understand how heme and zinc interact with each other and the binding sites on the channel itself. Since extracellular residue neutralization mutants have been shown to impact pH and zinc binding and modulation, we now need to look at how heme's effect is altered in these mutants. Following mutations in the clusters, zinc and heme concentrations should be increased to see if it the regulation of gating is completely disrupted or just significantly reduced.

Chapter 6

Final Thoughts

Overall the localization and channel functionality data presented evidence that dmElk channels are involved in the maintenance of subthreshold excitability in the putative AIS of *Drosophila melanogaster*. The localization data shows that dmElk is limited to the region associated with the AIS in *Drosophila*. It also shows that while something is keeping the channel there it is most likely not Ank2; however, the Dlg anchoring protein does seem to play a role in maintaining the location of this channel. The presence of dmElk in the putative AIS suggests that it plays a role in action potential regulation.

The GV curves suggest that dmElk and Elk1 channels open beneath threshold voltages and therefore most likely help maintain the subthreshold voltage value and regulate subthreshold excitability. The electrophysiology results also show that there is a complex regulation for the gating properties of Elk1. Heme seems to sensitize the channel to voltages through the removal of protons while zinc appears to desensitize the channel by blocking the pore. Heme and zinc clearly interact with each other in what seems to be an allosteric potentiation of zinc by heme, resulting in increased sensitivity of the channel to zinc's effect. It is important to note that heme and zinc do not have a proposed physiological mechanism in the light of this research and other molecules are most likely responsible for gating regulation in organisms in relation to the external charge cluster.

The data presented within this thesis provides more information regarding the proteins maintaining and present in the putative AIS of *Drosophila melanogaster* while also suggesting

that the dmElk channels present help maintain subthreshold voltages, playing a crucial role in action potential regulation.

References

Albertson, R., & Doe, C. Q. (2003). Dlg, Scrib and Lgl regulate neuroblast cell size and mitotic spindle asymmetry. *Nat Cell Biol, 5*(2), 166-170. doi:10.1038/ncb922

Astorga, C., Jorquera, R. A., Ramirez, M., Kohler, A., Lopez, E., Delgado, R., . . . Sierralta, J. (2016). Presynaptic DLG regulates synaptic function through the localization of voltage-activated Ca(2+) Channels. *Sci Rep, 6*, 32132. doi:10.1038/srep32132

Bellen, H. J., Tong, C., & Tsuda, H. (2010). 100 years of Drosophila research and its impact on vertebrate neuroscience: a history lesson for the future. *Nat Rev Neurosci, 11*(7), 514-522. doi:10.1038/nrn2839

Beller, M., & Oliver, B. (2006). One hundred years of high-throughput Drosophila research. *Chromosome Res, 14*(4), 349-362. doi:10.1007/s10577-006-1065-2

Bender, K. J., & Trussell, L. O. (2009). Axon initial segment Ca2+ channels influence action potential generation and timing. *Neuron, 61*(2), 259-271. doi:10.1016/j.neuron.2008.12.004

Bender, K. J., & Trussell, L. O. (2012). The physiology of the axon initial segment. *Annu Rev Neurosci, 35*, 249-265. doi:10.1146/annurev-neuro-062111-150339

Bennett, V., & Baines, A. J. (2001). Spectrin and ankyrin-based pathways: metazoan inventions for integrating cells into tissues. *Physiol Rev, 81*(3), 1353-1392. doi:10.1152/physrev.2001.81.3.1353

Bennett, V., & Lorenzo, D. N. (2013). Spectrin- and ankyrin-based membrane domains and the evolution of vertebrates. *Curr Top Membr, 72*, 1-37. doi:10.1016/b978-0-12-417027-8.00001-5

Berghs, S., Aggujaro, D., Dirkx, R., Jr., Maksimova, E., Stabach, P., Hermel, J. M., . . . Solimena, M. (2000). betaIV spectrin, a new spectrin localized at axon initial segments and nodes of ranvier in the central and peripheral nervous system. *J Cell Biol, 151*(5), 985-1002.

Bernsteiner, H., Brundl, M., & Stary-Weinzinger, A. (2017). Dynamics of the EAG1 K(+) channel selectivity filter assessed by molecular dynamics simulations. *Biochem Biophys Res Commun, 484*(1), 107-112. doi:10.1016/j.bbrc.2017.01.064

Bilder, D., Li, M., & Perrimon, N. (2000). Cooperative regulation of cell polarity and growth by Drosophila tumor suppressors. *Science, 289*(5476), 113-116.

Brachet, A., Leterrier, C., Irondelle, M., Fache, M. P., Racine, V., Sibarita, J. B., . . . Dargent, B. (2010). Ankyrin G restricts ion channel diffusion at the axonal initial segment before the establishment of the diffusion barrier. *J Cell Biol, 191*(2), 383-395. doi:10.1083/jcb.201003042

Chen, K., & Featherstone, D. E. (2005). Discs-large (DLG) is clustered by presynaptic innervation and regulates postsynaptic glutamate receptor subunit composition in Drosophila. *BMC Biol, 3*, 1. doi:10.1186/1741-7007-3-1

Davis, L., Abdi, K., Machius, M., Brautigam, C., Tomchick, D. R., Bennett, V., & Michaely, P. (2009). Localization and structure of the ankyrin-binding site on beta2-spectrin. *J Biol Chem, 284*(11), 6982-6987. doi:10.1074/jbc.M809245200

Debattisti, V., & Scorrano, L. (2013). D. melanogaster, mitochondria and neurodegeneration: small model organism, big discoveries. *Mol Cell Neurosci, 55*, 77-86. doi:10.1016/j.mcn.2012.08.007

Dietzl, G., Chen, D., Schnorrer, F., Su, K. C., Barinova, Y., Fellner, M., . . . Dickson, B. J. (2007). A genome-wide transgenic RNAi library for conditional gene inactivation in Drosophila. *Nature, 448*(7150), 151-156. doi:10.1038/nature05954

Drummond, D. R., Armstrong, J., & Colman, A. (1985). The effect of capping and polyadenylation on the stability, movement and translation of synthetic messenger RNAs in Xenopus oocytes. *Nucleic Acids Res, 13*(20), 7375-7394.

Evans, M. D., Sammons, R. P., Lebron, S., Dumitrescu, A. S., Watkins, T. B., Uebele, V. N., . . . Grubb, M. S. (2013). Calcineurin signaling mediates activity-dependent relocation of the axon initial segment. *J Neurosci, 33*(16), 6950-6963. doi:10.1523/jneurosci.0277-13.2013

Fire, A., Xu, S., Montgomery, M. K., Kostas, S. A., Driver, S. E., & Mello, C. C. (1998). Potent and specific genetic interference by double-stranded RNA in Caenorhabditis elegans. *Nature, 391*(6669), 806-811. doi:10.1038/35888

Frolov, R. V., Bagati, A., Casino, B., & Singh, S. (2012). Potassium channels in Drosophila: historical breakthroughs, significance, and perspectives. *J Neurogenet, 26*(3-4), 275-290. doi:10.3109/01677063.2012.744990

Gan, G., & Zhang, C. (2018). The precise subcellular localization of Dlg in the Drosophila larva body wall using improved pre-embedding immuno-EM. *J Neurosci Res, 96*(3), 467-480. doi:10.1002/jnr.24139

Garrido, J. J., Giraud, P., Carlier, E., Fernandes, F., Moussif, A., Fache, M. P., . . . Dargent, B. (2003). A targeting motif involved in sodium channel clustering at the axonal initial segment. *Science, 300*(5628), 2091-2094. doi:10.1126/science.1085167

Giovane, A., Sobieszczuk, P., Mignon, C., Mattei, M. G., & Wasylyk, B. (1995). Locations of the ets subfamily members net, elk1, and sap1 (ELK3, ELK1, and ELK4) on three homologous regions of the mouse and human genomes. *Genomics, 29*(3), 769-772. doi:10.1006/geno.1995.9938

Grueber, W. B., Jan, L. Y., & Jan, Y. N. (2002). Tiling of the Drosophila epidermis by multidendritic sensory neurons. *Development, 129*(12), 2867-2878.

Harindranath, N., Mills, F. C., Mitchell, M., Meindl, A., & Max, E. E. (1998). The human elk-1 gene family: the functional gene and two processed pseudogenes embedded in the IgH locus. *Gene, 221*(2), 215-224.

Hill, A. S., Nishino, A., Nakajo, K., Zhang, G., Fineman, J. R., Selzer, M. E., . . . Cooper, E. C. (2008). Ion channel clustering at the axon initial segment and node of Ranvier evolved sequentially in early chordates. *PLoS Genet, 4*(12), e1000317. doi:10.1371/journal.pgen.1000317

Hough, C. D., Woods, D. F., Park, S., & Bryant, P. J. (1997). Organizing a functional junctional complex requires specific domains of the Drosophila MAGUK Discs large. *Genes Dev, 11*(23), 3242-3253.

Jegla, T., Grigoriev, N., Gallin, W. J., Salkoff, L., & Spencer, A. N. (1995). Multiple Shaker potassium channels in a primitive metazoan. *J Neurosci, 15*(12), 7989-7999.

Jegla, T., Marlow, H. Q., Chen, B., Simmons, D. K., Jacobo, S. M., & Martindale, M. Q. (2012). Expanded functional diversity of shaker K(+) channels in cnidarians is driven by gene expansion. *PLoS One, 7*(12), e51366. doi:10.1371/journal.pone.0051366

Jegla, T., Nguyen, M. M., Feng, C., Goetschius, D. J., Luna, E., van Rossum, D. B., . . . Rolls, M. M. (2016). Bilaterian Giant Ankyrins Have a Common Evolutionary Origin and Play a Conserved Role in Patterning the Axon Initial Segment. doi:10.1371/journal.pgen.1006457

Jegla, T., Nguyen, M. M., Feng, C., Goetschius, D. J., Luna, E., van Rossum, D. B., . . . Rolls, M. M. (2018). Bilaterian Giant Ankyrins Have a Common Evolutionary Origin and Play a Conserved Role in Patterning the Axon Initial Segment. doi:10.1371/journal.pgen.1006457

Jegla, T., & Salkoff, L. (1994). Molecular evolution of K+ channels in primitive eukaryotes. *Soc Gen Physiol Ser, 49*, 213-222.

Jegla, T., & Salkoff, L. (1997). A novel subunit for shal K+ channels radically alters activation and inactivation. *J Neurosci, 17*(1), 32-44.

Jegla, T. J., Zmasek, C. M., Batalov, S., & Nayak, S. K. (2009). Evolution of the human ion channel set. *Comb Chem High Throughput Screen, 12*(1), 2-23.

Jenkins, P. M., Kim, N., Jones, S. L., Tseng, W. C., Svitkina, T. M., Yin, H. H., & Bennett, V. (2015). Giant ankyrin-G: a critical innovation in vertebrate evolution of fast and integrated neuronal signaling. *Proc Natl Acad Sci U S A, 112*(4), 957-964. doi:10.1073/pnas.1416544112

Jensen, M. S., & Yaari, Y. (1997). Role of intrinsic burst firing, potassium accumulation, and electrical coupling in the elevated potassium model of hippocampal epilepsy. *J Neurophysiol, 77*(3), 1224-1233. doi:10.1152/jn.1997.77.3.1224

Jones, S. L., Korobova, F., & Svitkina, T. (2014). Axon initial segment cytoskeleton comprises a multiprotein submembranous coat containing sparse actin filaments. *J Cell Biol, 205*(1), 67-81. doi:10.1083/jcb.201401045

Jones, S. L., & Svitkina, T. M. (2016). Axon Initial Segment Cytoskeleton: Architecture, Development, and Role in Neuron Polarity. *Neural Plast, 2016*, 6808293. doi:10.1155/2016/6808293

Kalstrup, T., & Blunck, R. (2018). S4-S5 linker movement during activation and inactivation in voltage-gated K(+) channels. *Proc Natl Acad Sci U S A, 115*(29), E6751-e6759. doi:10.1073/pnas.1719105115

Karim, M. R., & Moore, A. W. (2011). Morphological analysis of Drosophila larval peripheral sensory neuron dendrites and axons using genetic mosaics. *J Vis Exp*(57), e3111. doi:10.3791/3111

Kazmierczak, M., Zhang, X., Chen, B., Mulkey, D. K., Shi, Y., Wagner, P. G., . . . Jegla, T. (2013). External pH modulates EAG superfamily K+ channels through EAG-specific acidic residues in the voltage sensor. *J Gen Physiol, 141*(6), 721-735. doi:10.1085/jgp.201210938

Kobayashi, T., Storrie, B., Simons, K., & Dotti, C. G. (1992). A functional barrier to movement of lipids in polarized neurons. *Nature, 359*(6396), 647-650. doi:10.1038/359647a0

Koch, I., Schwarz, H., Beuchle, D., Goellner, B., Langegger, M., & Aberle, H. (2008). Drosophila ankyrin 2 is required for synaptic stability. *Neuron, 58*(2), 210-222. doi:10.1016/j.neuron.2008.03.019

Kole, M. H., Ilschner, S. U., Kampa, B. M., Williams, S. R., Ruben, P. C., & Stuart, G. J. (2008). Action potential generation requires a high sodium channel density in the axon initial segment. *Nat Neurosci, 11*(2), 178-186. doi:10.1038/nn2040

Kole, M. H., Letzkus, J. J., & Stuart, G. J. (2007). Axon initial segment Kv1 channels control axonal action potential waveform and synaptic efficacy. *Neuron, 55*(4), 633-647. doi:10.1016/j.neuron.2007.07.031

Kordeli, E., Lambert, S., & Bennett, V. (1995). AnkyrinG. A new ankyrin gene with neural-specific isoforms localized at the axonal initial segment and node of Ranvier. *J Biol Chem, 270*(5), 2352-2359.

Lee, J., Ueda, A., & Wu, C. F. (2014). Distinct roles of Drosophila cacophony and Dmca1D Ca(2+) channels in synaptic homeostasis: genetic interactions with slowpoke Ca(2+) -activated BK channels in presynaptic excitability and postsynaptic response. *Dev Neurobiol, 74*(1), 1-15. doi:10.1002/dneu.22120

Lemaillet, G., Walker, B., & Lambert, S. (2003). Identification of a conserved ankyrin-binding motif in the family of sodium channel alpha subunits. *J Biol Chem, 278*(30), 27333-27339. doi:10.1074/jbc.M303327200

Leterrier, C., Potier, J., Caillol, G., Debarnot, C., Rueda Boroni, F., & Dargent, B. (2015). Nanoscale Architecture of the Axon Initial Segment Reveals an Organized and Robust Scaffold. *Cell Rep, 13*(12), 2781-2793. doi:10.1016/j.celrep.2015.11.051

Li, X., Anishkin, A., Liu, H., van Rossum, D. B., Chintapalli, S. V., Sassic, J. K., . . . Jegla, T. (2015). Bimodal regulation of an Elk subfamily K+ channel by phosphatidylinositol 4,5-bisphosphate. *J Gen Physiol, 146*(5), 357-374. doi:10.1085/jgp.201511491

Li, X., Liu, H., Chu Luo, J., Rhodes, S. A., Trigg, L. M., van Rossum, D. B., . . . Jegla, T. (2015). Major diversification of voltage-gated K+ channels occurred in ancestral parahoxozoans. *Proc Natl Acad Sci U S A, 112*(9), E1010-1019. doi:10.1073/pnas.1422941112

Li, X., Martinson, A. S., Layden, M. J., Diatta, F. H., Sberna, A. P., Simmons, D. K., . . . Jegla, T. J. (2015). Ether-a-go-go family voltage-gated K+ channels evolved in an ancestral metazoan and functionally diversified in a cnidarian-bilaterian ancestor. *J Exp Biol, 218*(Pt 4), 526-536. doi:10.1242/jeb.110080

Liman, E. R., Hess, P., Weaver, F., & Koren, G. (1991). Voltage-sensing residues in the S4 region of a mammalian K+ channel. *Nature, 353*(6346), 752-756. doi:10.1038/353752a0

Nakada, C., Ritchie, K., Oba, Y., Nakamura, M., Hotta, Y., Iino, R., . . . Kusumi, A. (2003). Accumulation of anchored proteins forms membrane diffusion barriers during neuronal polarization. *Nat Cell Biol, 5*(7), 626-632. doi:10.1038/ncb1009

Nanoject II Auto-Nanoliter Injector. (2019).

Nelson, A. D., & Jenkins, P. M. (2017). Axonal Membranes and Their Domains: Assembly and Function of the Axon Initial Segment and Node of Ranvier. *Front Cell Neurosci, 11*, 136. doi:10.3389/fncel.2017.00136

Ogawa, Y., Horresh, I., Trimmer, J. S., Bredt, D. S., Peles, E., & Rasband, M. N. (2008). Postsynaptic density-93 clusters Kv1 channels at axon initial segments independently of Caspr2. *J Neurosci, 28*(22), 5731-5739. doi:10.1523/JNEUROSCI.4431-07.2008

Palay, S. L., Sotelo, C., Peters, A., & Orkand, P. M. (1968). The axon hillock and the initial segment. *J Cell Biol, 38*(1), 193-201.

Pan, Z., Kao, T., Horvath, Z., Lemos, J., Sul, J. Y., Cranstoun, S. D., . . . Cooper, E. C. (2006). A common ankyrin-G-based mechanism retains KCNQ and NaV channels at electrically active domains of the axon. *J Neurosci, 26*(10), 2599-2613. doi:10.1523/jneurosci.4314-05.2006

Panchal, K., & Tiwari, A. K. (2017). Drosophila melanogaster "a potential model organism" for identification of pharmacological properties of plants/plant-derived components. *Biomed Pharmacother, 89*, 1331-1345. doi:10.1016/j.biopha.2017.03.001

Peng, I. F., & Wu, C. F. (2007). Drosophila cacophony channels: a major mediator of neuronal Ca2+ currents and a trigger for K+ channel homeostatic regulation. *J Neurosci, 27*(5), 1072-1081. doi:10.1523/jneurosci.4746-06.2007

Pielage, J., Cheng, L., Fetter, R. D., Carlton, P. M., Sedat, J. W., & Davis, G. W. (2008). A presynaptic giant ankyrin stabilizes the NMJ through regulation of presynaptic microtubules and transsynaptic cell adhesion. *Neuron, 58*(2), 195-209. doi:10.1016/j.neuron.2008.02.017

Rasband, M. N. (2010). The axon initial segment and the maintenance of neuronal polarity. *Nat Rev Neurosci, 11*(8), 552-562. doi:10.1038/nrn2852

Rieckhof, G. E., Yoshihara, M., Guan, Z., & Littleton, J. T. (2003). Presynaptic N-type calcium channels regulate synaptic growth. *J Biol Chem, 278*(42), 41099-41108. doi:10.1074/jbc.M306417200

Rolls, M. *Welcome to the Rolls lab!*

Rolls, M. M. (2011). Neuronal polarity in Drosophila: sorting out axons and dendrites. *Dev Neurobiol, 71*(6), 419-429. doi:10.1002/dneu.20836

Rolls, M. M., Satoh, D., Clyne, P. J., Henner, A. L., Uemura, T., & Doe, C. Q. (2007). Polarity and intracellular compartmentalization of Drosophila neurons. *Neural Dev, 2*, 7. doi:10.1186/1749-8104-2-7

Saras, A., & Tanouye, M. A. (2016). Mutations of the Calcium Channel Gene cacophony Suppress Seizures in Drosophila. *PLoS Genet, 12*(1), e1005784. doi:10.1371/journal.pgen.1005784

Shah, M. M., Migliore, M., Valencia, I., Cooper, E. C., & Brown, D. A. (2008). Functional significance of axonal Kv7 channels in hippocampal pyramidal neurons. *Proc Natl Acad Sci U S A, 105*(22), 7869-7874. doi:10.1073/pnas.0802805105

Shu, Y., Yu, Y., Yang, J., & McCormick, D. A. (2007). Selective control of cortical axonal spikes by a slowly inactivating K+ current. *Proc Natl Acad Sci U S A, 104*(27), 11453-11458. doi:10.1073/pnas.0702041104

Silverman, W. R., Bannister, J. P., & Papazian, D. M. (2004). Binding site in eag voltage sensor accommodates a variety of ions and is accessible in closed channel. *Biophys J, 87*(5), 3110-3121. doi:10.1529/biophysj.104.044602

Silverman, W. R., Roux, B., & Papazian, D. M. (2003). Structural basis of two-stage voltage-dependent activation in K+ channels. *Proc Natl Acad Sci U S A, 100*(5), 2935-2940. doi:10.1073/pnas.0636603100

Silverman, W. R., Tang, C. Y., Mock, A. F., Huh, K. B., & Papazian, D. M. (2000). Mg(2+) modulates voltage-dependent activation in ether-a-go-go potassium channels by binding between transmembrane segments S2 and S3. *J Gen Physiol, 116*(5), 663-678.

Song, A. H., Wang, D., Chen, G., Li, Y., Luo, J., Duan, S., & Poo, M. M. (2009). A selective filter for cytoplasmic transport at the axon initial segment. *Cell, 136*(6), 1148-1160. doi:10.1016/j.cell.2009.01.016

Stoler, O., & Fleidervish, I. A. (2016). Functional implications of axon initial segment cytoskeletal disruption in stroke. *Acta Pharmacol Sin, 37*(1), 75-81. doi:10.1038/aps.2015.107

Tardi, N. J., Cook, M. E., & Edwards, K. A. (2012). Rapid phenotypic analysis of uncoated Drosophila samples with low-vacuum scanning electron microscopy. *Fly (Austin), 6*(3), 184-192. doi:10.4161/fly.20525

Trunova, S., Baek, B., & Giniger, E. (2011). Cdk5 regulates the size of an axon initial segment-like compartment in mushroom body neurons of the Drosophila central brain. *J Neurosci, 31*(29), 10451-10462. doi:10.1523/jneurosci.0117-11.2011

User Guide: mMESSAGE mMACHINE SP6 Transcription Kit. (2019). Retrieved from https://www.thermofisher.com/order/catalog/product/AM1340

Wang, S., Yang, J., Tsai, A., Kuca, T., Sanny, J., Lee, J., . . . Krieger, C. (2011). Drosophila adducin regulates Dlg phosphorylation and targeting of Dlg to the synapse and epithelial membrane. *Dev Biol, 357*(2), 392-403. doi:10.1016/j.ydbio.2011.07.010

Warmke, J. W., & Ganetzky, B. (1994). A family of potassium channel genes related to eag in Drosophila and mammals. *Proc Natl Acad Sci U S A, 91*(8), 3438-3442.

Whicher, J. R., & MacKinnon, R. (2016). Structure of the voltage-gated K(+) channel Eag1 reveals an alternative voltage sensing mechanism. *Science, 353*(6300), 664-669. doi:10.1126/science.aaf8070

Winckler, B., Forscher, P., & Mellman, I. (1999). A diffusion barrier maintains distribution of membrane proteins in polarized neurons. *Nature, 397*(6721), 698-701. doi:10.1038/17806

Woods, D. F., Hough, C., Peel, D., Callaini, G., & Bryant, P. J. (1996). Dlg protein is required for junction structure, cell polarity, and proliferation control in Drosophila epithelia. *J Cell Biol, 134*(6), 1469-1482.

Xu, K., Zhong, G., & Zhuang, X. (2013). Actin, spectrin, and associated proteins form a periodic cytoskeletal structure in axons. *Science, 339*(6118), 452-456. doi:10.1126/science.1232251

Yang, Y., Ogawa, Y., Hedstrom, K. L., & Rasband, M. N. (2007). betaIV spectrin is recruited to axon initial segments and nodes of Ranvier by ankyrinG. *J Cell Biol, 176*(4), 509-519. doi:10.1083/jcb.200610128

Zhang, X., Bertaso, F., Yoo, J. W., Baumgärtel, K., Clancy, S. M., Lee, V., . . . Jegla, T. (2010). Deletion of the potassium channel Kv12.2 causes hippocampal hyperexcitability and epilepsy. *Nat Neurosci, 13*(9), 1056-1058. doi:10.1038/nn.2610

Zhang, X., Bursulaya, B., Lee, C. C., Chen, B., Pivaroff, K., & Jegla, T. (2009). Divalent cations slow activation of EAG family K+ channels through direct binding to S4. *Biophys J, 97*(1), 110-120. doi:10.1016/j.bpj.2009.04.032

Zou, A., Lin, Z., Humble, M., Creech, C. D., Wagoner, P. K., Krafte, D., . . . Wickenden, A. D. (2003). Distribution and functional properties of human KCNH8 (Elk1) potassium channels. *Am J Physiol Cell Physiol, 285*(6), C1356-1366. doi:10.1152/ajpcell.00179.2003

Appendix

Drosophila melanogaster Genetic Plan